Wayne State University Dissertations

1-1-2014

Uracil Accumulation Response To Folate Depletion Is A Function Of Dna Repair Imbalance That May Be A Mechanism Of Aging

Hongzhi Ma
Wayne State University,

Recommended Citation

**URACIL ACCUMULATION RESPONSE TO FOLATE DEPLETION IS A
FUNCTION OF DNA REPAIR IMBALANCE THAT MAY BE A MECHANISM OF
AGING**

by

HONGZHI MA

DISSERTATION

Submitted to the Graduate School

of Wayne State University,

Detroit, Michigan

in partial fulfillment of the requirements

for the degree of

DOCTOR OF PHILOSOPHY

2014

MAJOR: NUTRITION & FOOD SCIENCE

Approved by:

_____

 Advisor   Date

_____

_____

_____

_____

ACKNOWLEDGEMENTS

I would like to thank my advisor Dr. Diane Cabelof for being both my mentor and my friend. Words cannot fully express how greatly I appreciate all that she has done for me, as she has helped me not only to develop as an independent scientist but also an independent woman. I would also like to thank the members of my dissertation committee, Dr. Ahmad Heydari, Dr. Kequan Zhou, and Dr. James Tucker for all their time, help, guidance and advice.

I would like to thank all of the present and past members of the Diane laboratory for their friendship, instruction and support—especially Kirk Simon, Yizhen Wu, Ghada Aoun, Eneida Doko, Aqila Ahmed, Denise Barak, Sarah Dubaisi, Alina Hall and Dr. Rita Rosati. I would also thank the Nutrition & Food Science departmental staff for all of their work on my behalf over the years.

Finally, I would like to thank my family and friends for their constant support throughout my career. I especially thank my husband Meng for all his advice, support, patience, devotion, and most of all for his love and my two lovely kids, Tony and Karen, for their smiling, crying, everything and love to me.

TABLE OF CONTENTS

LIST OF TABLES

LIST OF FIGURES

CHAPTER 1

INTRODUCTION

Folate, folate deficiency and disease

Folate is the water soluble vitamin B9. It is an essential nutrient for humans. Humans can't synthesis folate *de novo.* It only can be taken from the foods where the folate is naturally synthesized, or from the supplements as the form of folic acid. The leafy vegetables are the principal source of folate. Folate also can be found in many different kinds of foods and the levels may vary significantly. The highest levels of folate are found in yeast, eggs, liver, green leafy vegetables, leguminous vegetables and certain fruits (Lucock 2000). Folate exists in reduced form and oxidized form. The reduced form polyglutamates are found in animal and plant foods. The fully oxidized form (folic acid) is not found naturally but it is the form used in supplements. The folic acid form of the vitamin has no biological function. It is absorbed through the intestinal epithelium and reduced to tetrahydrofolate (THF). THF and its derivatives have important biological functions during many reactions, like DNA synthesis, RNA synthesis, DNA methylation, DNA repair, cell division and growth.

People have studied folate for about one hundred years. Since the 1920's, people thought the folate status has a relationship with anemia (Lanska 2010). Later scientists found that folate in the brewer's yeast having prevention function to the anemia during the pregnancy. Folate was first extracted from spinach

leaves in 1941 (Mitchell, Snell et al. 1941). After many years of study, scientist discovered the linkage between folate deficiency and neural tube defects (Lanska 2010). In 1968, the value of folate deficiency was set (<3 ng/ml in serum, <100ng/ml in red blood cells) for the first time. Later that was used by the World Health Organization (WHO) in 1972 and 1975 (WHO 2012). When the USA government found the necessity to provide enough folate to meet the folate requirement, the folate fortification program was born in 1998 and now people can buy various kinds of fortified foods with folic acid from the grocery store.

In the middle of the last century, scientists began to study and learn the bio-function of folate. More and more mechanisms of folate were discovered, and more relationships between folate status and disease were identified.

Folic acid from the diet is absorbed in the small intestine, and is transported by the reduced folate carrier (RFC) through the cell membrane and into the cell. Then it is reduced to dihydrofolate. The product then is reduced by the enzyme dihydrofolate reductase (DHFR) to tetrahydrofolate (polyglutamate) using NADPH as an electron donor. The tetrahydrofolate with polyglutamate residue tail keeps it inside cells and makes it possible to perform the bio-functions in cells. When the polyglutamate tail is hydrolyzed by Gamma-glutamyl hydrolase (GGH), the molecule will be converted to monoglutamate, which may be transported through the cell membrane again. The monoglutamate folate also can be attached to multiple glutamate residues by the folypolyglutamate synthase (FPGS). This enzyme reaction is ATP-dependent and essential for the

folate homeostasis. Folate carries and transfers one carbon units, in which the enzyme serine hydroxymethyltransferase (SHMT) has a key role. SHMT catalyzes the conversions of serine to glycine and tetrahydrofolate to 5, 10-methylenetetrahydrofolate at the same time, and this reaction provides the most amount of one-carbon units available to the cell. SHMT1 and SHMT2 are the two isoforms; the first one is in the cytoplasm and the second one is in the mitochondria (Appaji Rao, Ambili et al. 2003). 5, 10-methylenetetrahydrofolate provides one carbon unit to dUMP and converts dUMP to dUTP. This reaction is catalyzed by the enzyme thymidylate synthetase (TS) and generates thymidylate for DNA synthesis and repair. 5, 10-methylenetetrahydrofolate also can be converted to 5-methyltetrahydrofolate by the enzyme methylenetetrahydrofolate reductase (MTHFR), and the products are involved in the homocysteine-methionine circle. In this reaction, 5-methylTHF is converted to THF, and methionine is synthesized by the methionine synthase (MTR). Methionine provides methyl groups for DNA methylation. The transsulfuration pathway of homocysteine to cysteine is catalyzed by the enzyme cystathionine-β-synthase (CBS) in the first step. The intermediate product is cystathionine. Due to the ability of thiols to undergo redox reactions, cysteine has antioxidant properties, and it is the precursor of the antioxidant glutathione. The whole mechanism process is shown in figure 1 (Shen, Rothman et al. 2005).

Folate carries and transfers one-carbon units among the biological function pathway. It plays an important role in nucleotide synthesis, DNA

methylation, and antioxidant action through homocysteine-cysteine. When folate status changes, the limited one-carbon units will have critical impact on those biological functions, which may result in various health problems, such as anemia and neural tube defects of infants (Lanska 2010). Folate may also have a role in the prevention of cardiovascular disease (CVD) by the regulation of the homocysteins (McNulty, Pentieva et al. 2008). Beside the effects of folate on the nucleotide synthesis, researchers also found that in human WIL2-NS cells folate deficiency results telomere shortening and dysfunction (Bull, Mayrhofer et al. 2014), and increasing of the frequency of binucleated cells with micronuclei and/or nucleoplasmic bridges (Beetstra, Thomas et al. 2005). Under the folate deficiency condition the fragile sites in chromosomes are expressed, and single- , double- DNA strand breaks, chromosome breakage and micronucleus (MN) expression are increased (Fenech 2001). Furthermore, many studies were done about the folate status and various cancers. There are different opinions on that. Higher dietary folate may reduce the risk of colorectal cancer and prostate cancer (Sanjoaquin, Allen et al. 2005, Johansson, Appleby et al. 2008). Other data show the folic acid fortification program increasing the risk of colorectal cancer within the population (Jennings and Willis 2014). Until now the mechanism of folate status with the disease is not all identified; there are many interesting mountains for us to climb.

DNA base excision repair (BER) and uracil DNA glycosylase

We know the importance of genetic variation in life, but the genetic stability is also important for the individual to survive. The genetic stability needs not only the extremely accurate replication of DNA, but also the remarkable mechanism of DNA repair. Due to various reasons such as heat, metabolic accidents, and environmental exposure, spontaneous changes in DNA happen every minute. But most of the changes are corrected by the mechanisms of DNA repair; other changes have less than 1 of 1000 chance to become permanent mutation in DNA (Alberts 2002).

DNA base excision repair (BER) is one of the multiple pathways of DNA repair. This pathway involves abundant DNA glycosylases, which targets deaminated cytosine (uracil), deaminated adenine, different types of alkylated or oxidized bases, bases with opened rings, and bases in which a carbon-carbon double bond has been accidentally converted to a carbon-carbon single bond (Alberts 2002). For example, the deaminated cytosine (uracil) is removed by uracil DNA glycosylase through the hydrolytic catalyzation and generates an AP site (apurinic/apyrimidinic site), also known as an abasic site. Then the AP endonuclease and a phosphodiesterase cut off the sugar phosphate and generate a single strand break. DNA polymerase (β-pol) attaches a correct nucleotide and DNA ligase III along with its cofactor XRCC1 seals the nick. So the result is that misincorparated uracil is replaced by cytosine (Alberts 2002).

DNA glycosylases are the key enzymes to remove uracil during BER. Based on the different substrates and subcellular localization, there are four

major types of DNA glycosylases. They are Uracil-N glycosylase (Ung), single-strand-specific monofunctional uracil DNA glycosylase1 (Smug1), Methyl-binding domain glycosylase 4 (Mbd4) and Thymine DNA glycosylase (Tdg). All of them are monofunctional, which means they only remove the damaged base from the sugar, they don't cut off the sugar phosphate. The substrate of UNG is uracil, deaminated from cytosine or misincorporated dU opposite dA during DNA replication, in both single strand and double strand DNA.(Jacobs and Schar 2012). SMUG1 was found to serve as back-up for UNG in limiting the deaminated cytosine (U:G) and misincorporated uracil (U:A) (An, Robins et al. 2005). MBD4 and TDG are involved in the pyrimidine derivates in mismatches including U, 5-FU et al. in dsDNA (Jacobs and Schar 2012). In this study, we evaluate these enzymes' gene expression level under the folate deficiency condition and the UDG activity, BER activity, and try to disclose the key mechanism behind the uracil accumulation response to folate depletion.

Folate deficiency, uracil accumulation in DNA and Aging

Folate deficiency will limit the one-carbon units in human body; one of the results is the impact on the uracil miscorporation in DNA. That has been evidenced in some studies. In 1999, the Duthie group found a 2-3 fold uracil level increase in human lymphocytes with folate deficient medium (Duthie 1999). In 1997, Blount found an 8 fold uracil level greater than control group in human whole blood (Blount, Mack et al. 1997). In 2008, Kronenberg found uracil level elevated in homogenates of whole cerebral hemispheres of *Ung -/-* compared

with *Ung* +/+ mice and that was further increased by folate deficiency. They indicated impaired uracil repair is involved in neurodegeneration and neuropsychiatric dysfunction induced by experimental folate deficiency (Kronenberg, Harms et al. 2008). Our data also showed the uracil level increase in DNA from the aging colony of mice (Simon, Ma et al. 2012). The SEER cancer statistics review shows age is one of the strongest risk factors for colorectal cancer. Senior people have a high ratio of diagnoses (90% to 50 years old; 65.6% to >65 years old) (Ries 2007). Colorectal cancer is related to gene mutations, genome instability, and DNA strand break. One risk factor of colorectal cancer that has been widely studied is the reduced folate status. Both Herrmann and Choi found that folate status declines with age (Herrmann, Quast et al. 1999, Choi, Friso et al. 2003). Folate is involved in the DNA synthesis, DNA methylation, and antioxidant reaction. The limited folate may result in uracil accumulation in DNA, which may lead to gene mutation and genome instability. So we set up our hypothesis, **how the uracil accumulated in DNA response to the folate deficiency may be the same mechanism for aging.**

The role of the proteins coded by the genes in the folate and methylation metabolism circles
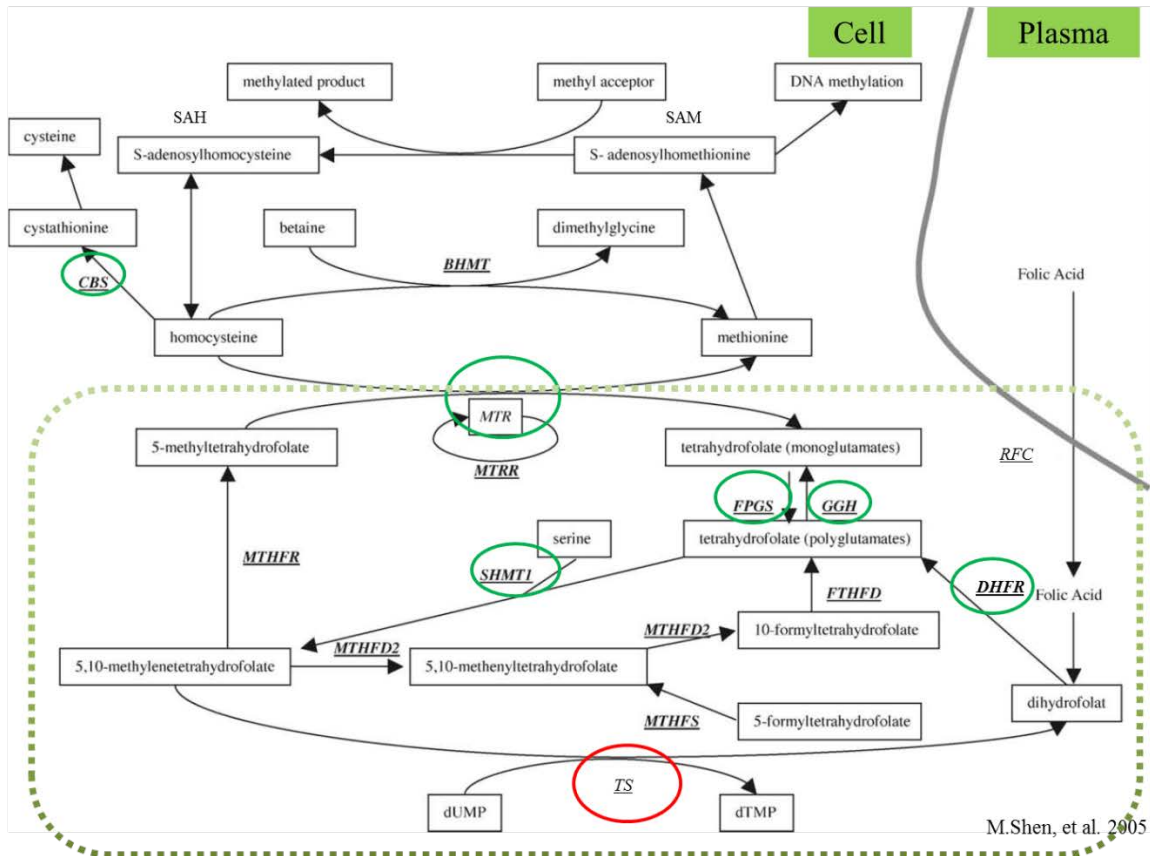
Figure1: The mechanism of folate involved in the DNA synthesis, DNA methylation, homocysteine-methionine circle.

CHAPTER 2

MODIFICATION AND OPTIMIZATION OF THE *LACTOBACILLUS CASEI*

MICROBIOLOGICAL FOLATE ASSAY AND ASSESSMENT OF

INTRACELLULAR AND TISSUE FOLATE LEVELS

INTRODUCTION

Folate, as a member of vitamin B group, is an important nutrient. As explained in Chapter 1, folate has various forms: reduced / oxidized forms, polyglutamates / monoglutamate forms. The oxidized form (folic acid) doesn't exist in the nature, but works as a food supplement. The reduced forms exist in the plants and animals, and are the bio-functional forms. The poly-/mono-glutamate forms make the difference of the transfer through the cell membrane and also have different bio-functions.

Folic acid is a conjugated molecule. It includes 3 parts: a pteridine ring, a para-aminobenzoic acid (PABA), and a glutamic acid residue(Blancquaert, Storozhenko et al. 2010). Animals cannot synthesize PABA nor attach glutamate residues to pteroic acid (Lucock 2000). So, dietary consumption of folate is required. Folate differs in the extent of polyglutamylation, oxidation state and type of one carbon unit attached to the N5, N10 positions. Folate carry and transfer various forms of one carbon units during biosynthetic reactions. The one carbon units are methyl (CH3), methylene (CH2), methenyl (CH), formyl (CHO) and formimino (CH=NH) groups (Figure 2) (Blancquaert, Storozhenko et al. 2010).

(Dominic Taylor)
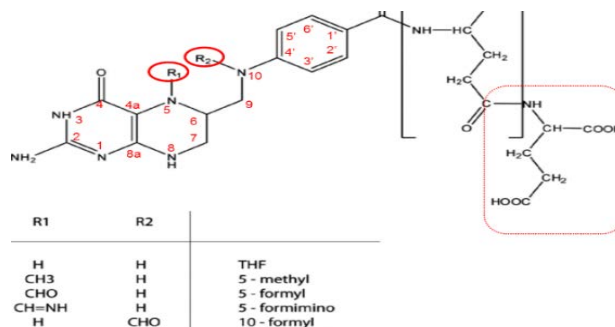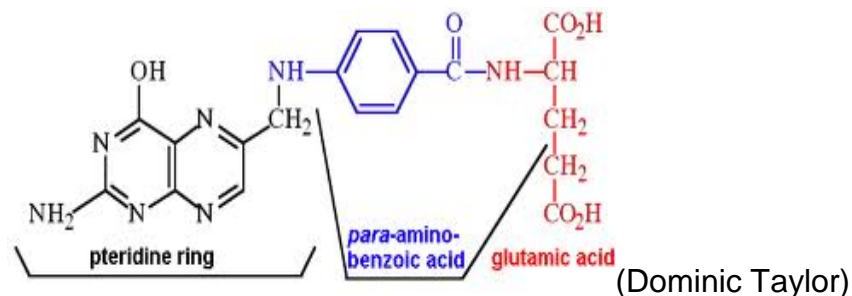
(Blancquaert, Storozhenko et al. 2010)

Figure 2: Folate molecular structure and one carbon units.

Folate carries and transfers one carbon units during biosynthetic reactions, such as nucleic acid synthesis, DNA methylation, and re-methylation of homocysteine to methionine. Folate deficiency may induce various kinds of human disease and symptoms, such as loss of appetite, weight loss, weakness, headaches, heart palpitations, behavioral disorders, anemia, and slow growth rate of children, low birth weight and premature infants, infants with neural tube defects, depression and tumorogenesis. Some studies have associated folate with Down's syndrome and Alzheimer's disease (Clarke, Smith et al. 1998, James, Pogribna et al. 1999). So it is important to determine the folate level to help evaluate risks for these diseases and help to prevent them as well.

A lot of studies have been done to determine the folate level through various methodologies, such as microbiological assay, competitive folate protein binding assays (the Bio-Rad (Hercules, CA) Quantaphase II radioimmunoassay and the Abbott (Abbott Park, IL) AxSYM Folate ions capture radioimmunoassay, folate (folic acid) ELISA kit) and recently developed mass spectrometry methods including HPLC, Liquid Chromatography-tandem MS (LC-MS/MS). But there are barriers during the interpretation between the different methods (Table 1).

The microbiological assay is the traditional method for determination of folate levels, and has been used to determine the folate levels in blood and red blood cells for over 50 years (Shane 2011). The microbiological assay is the gold standard for total folate status assessment. Later, the competitive folate protein binding assays were developed. These assays are desirable because they are easy to handle and the kits are commercially available, so they are widely used in clinical fields. But the disadvantage is that the folate concentrations obtained with these kits are typically lower than those from microbiological assay and showed large variations between different assay kits. When the kits are discontinued, we can't compare the longitudinal data. More recently, mass spectrometry methods have been developed that made it possible to determine the individual folate form level. The advantage is that it makes the possibility to observe the distribution of different forms of folate. However, the disadvantage is that these new methods need sophisticated instrumentation and complicated procedures. Another disadvantage is that the different folate forms may

interconvert into each other during the process. So, the results obtained from different methods have inconsistency, especially for one specific form of folate.

The microbiological folate assay has long been used. One disadvantage is that it doesn't distinguish between forms. We can't get distribution data of different folate forms through microbiological assay, but only the total folate level. Further, the *Lactobacillus casei* strain's growth depends on the concentration of monoglutamate form. The polyglutamate forms need to be hydrolyzed to monoglutamate by a conjugase. The efficiency of the enzyme will affect the final total concentration of folate. When labs use different conjugase or under different condition, there will be variations among the results. However the microbiological assay has many advantages: simplicity of operation, economy of reagents, quickness, sensitivity to low amount of folate and clear results. And it is suitable for the detection of total folate, which is good for our lab to define the folate adequate or folate deficiency status. We used the microbiological folate assay as described previously (Horne and Patterson 1988) in our project. Additionally, we optimized the assay condition and calculated the conjugase efficiency, and compared the different tissue folate levels.

MATERIALS AND METHODS

Cell culture & Animals

The intracellular folate levels were evaluated in two distinct cell types: SV-40 transformed mouse embryonic fibroblasts (MEFs; Tag 92) and BNL CL.2

cells, which are transformed liver cells derived from BALB/c mice (ATCC TIB-73TM). Cells were maintained in either folate-adequate or folate-free media (DMEM, Dulbecco's Modified Eagle Medium, gibco by Life technologies) with dialyzed Fetal bovine serum. Initially, cells grown in folate-free media were cultured in media supplemented with 10µM thymidine/60µM adenosine (T/A) that match the folate repletion condition to allow cell survival (Courtemanche, Elson-Schwab et al. 2004). Removal of folate from the media without T/A supplementation initially resulted in cell death. Stepwise reductions in the percent of T/A was conducted over time, such that T/A concentrations were decreased every 3 passages until T/A supplementation was not required for survival. Cells in both folate groups were ultimately harvested in the absence of exogenous T/A. Cells were counted using TC10 Automated Cell Counter, (Biorad, Hercules, CA) and were seeded at identical densities. Cells are harvested by trypsinization, centrifuged, washed with 1X PBS, flash frozen in liquid nitrogen and stored at -80° C for future analysis.

Mouse blood was used to optimize assay conditions in a relevant biological system and the blood samples were provided by Dr. Ahmad Heydari from Wayne State University. The mice are young (3–4 month), wild-type male C57BL/6 specific pathogen-free mice housed in accordance with NIH guidelines for the use and care of laboratory animals. The Wayne State University Animal Investigation Committee approved the animal protocol. The mice were maintained on a 12-hr light/dark cycle and fed standard mouse chow and water

ad libitum. At 3–4 months of age, the mice were randomly assigned to two dietary groups and were fed AIN93G-purified isoenergetic diets (Dyets, Inc., Lehigh Valley, PA). Diets were stored at −20°C. 1% succinyl sulfathiazole was added to all diets to kill intestinal bacteria that are able to synthesize folate (Said, Chatterjee et al. 2000). The control group received a folate adequate diet containing 2 mg/kg folic acid. The experimental group received a folate-deficient diet containing 0 mg/kg folic acid. The animals' food intake and body weights were monitored twice weekly to monitor for signs of toxicity (e.g., weight loss) (Unnikrishnan, Prychitko et al. 2011).

In order to evaluate tissue folate status, mouse tissue samples were obtained from Dr. Richard A. Miller's lab from the University of Michigan in Ann Arbor. BALB/cByJ3C57BL/6J F1 (CB6F1) females and C3H/HeJ3DBA/2J F1 (C3D2F1) males were mated to produce genetically heterogeneous populations in which each animal was genetically unique, but a full sibling of all other mice in the population (Harrison, Strong et al. 2009). Mice were anesthetized in a CO_2 chamber and sacrificed by cervical dislocation. Harvested tissues (liver, kidney, testis, small intestine, colon, brain) were flash frozen and stored in liquid nitrogen at the University of Michigan in Ann Arbor, and were taken to Wayne State University for folate analysis.

Extraction of Folate

Mouse Serum

Blood samples were obtained from the orbital sinus of mice by a sterile microhematocrit blood tube. Blood samples were clotted at room temperature for at least 30 minutes. They were centrifuged at 7000rpm for 15 minutes. We then transferred the supernatant (serum) to a new 1.5ml tube and added 3vol Buffer #1(0.25M sucrose, 10mM HEPES, 10mM 2 –mercaptoethanol, 10mM ascorbic acid). They were centrifuged at 12,000 rpm for 30 minutes. We transferred the supernatant to another new 1.5 new tube and added 0.2vol of Buffer #2(10% w/v ascorbic acid, 1M 2-mercaptoethanol, 0.25M HEPES, 0.25M CHES). Then we incubated them in the boiling water bath for 5 minutes. They were centrifuged at 12,000rpm for 5 minutes. We transferred the supernatant to a new tube for folate determination.

Cell / Mouse tissue

The following descriptions are suitable for cells or animal tissues. The cell pellets were collected with cell number counted; the mouse tissue were collected with the weight measured. Then the samples were added 10vol Buffer #1, and homogenized (Pellet pestle Motor, Kontes) 20 times or until the solution is consistent. Samples centrifuged at 12000rpm for 30 min, and the supernatant was transferred to a new tube and 0.2 volume Buffer #2 was added. Then they were incubated in the boiling water bath for 5 minutes and centrifuged at 12,000rpm for 5 minutes. The supernatant was transferred for conjugase treatment. We use chicken pancreas as conjugase to catalyze the conversion from polyglutamate folate to monoglutamate form. *Lactobacillus casei*'s growth

depends on the concentration of monoglutamate form. So 20µl of conjugase (chicken pancreas powder lyophilized, Pel-Freez, Rogers, Arkansas) and 80µl of Buffer #1 were added to the supernatant. The control should consist of 160 µl of Buffer #1, 20µl conjugase, and 20µl Buffer #2. Tubes were incubated in a 32ºC water bath for four hours. Then flash freeze the samples, and store the tubes in -80 ºC for folate microbiological assay use.

Overview of the *Lactobacillus casei* Microbiological Folate Assay

Before setting up the folate assay, we treated the cell pellets with the methods described above. Intracellular folate level is measured using the *Lactobacillus casei* (ATCC 7469) microbiological assay, described by Home et al (Horne and Patterson 1988). The bacteria, *Lactobacillus casei's* (*L. casei*) growth depends on the folate concentration. There is a linear relationship between them. When there are more folate in the growth media, the bacteria grow fast. We use the growth curve of the bacteria to measure the folate concentration in our samples.

Briefly, *L. casei* is cultured overnight in growth media (4.7% w/v solution Folic Acid Casei Medium, DifcoTM, Becton Dickinson, Sparks, MD) supplemented with 0.025% sodium ascorbate and 0.6µg/L folinic acid calcium salt (Santa Cruz, Santa Cruz, CA) to an OD of 0.05. The 300 µl reaction mixture contains 150µl media (9.4% solution Folic Acid Casei Medium, DifcoTM Becton Dickinson, Sparks, MD; 0.05% w/v sodium ascorbate), 8µl working buffer (0.16% w/v sodium ascorbate; 0.05mol/L potassium phosphate, pH 6.1), cell lysate (1µl,

2µl and 10µl for each sample) or the folinic acid calcium salt as standard (0, 10,20,40,60,80,100,120fmol in each well) , and at the end load 20µl *L.casei* at OD=0.05. A range of lysate volumes are used to ensure the data fall within the standard curve range. Sterile water is used to adjust the final volume to 300µl. The light-sensitive samples are covered and incubated at 37˚C for 21hrs. Absorbance is read at 595nm using a Genios Basic TECAN-GENios plus plate reader and TECAN Magellan v6.00 software (Tecan Group Ltd., Zurich, Switzerland). Folate concentration is calculated by comparing with standard. Folate concentration is considered significantly different from control at a p-value < 0.05.

Creation of Standard

We use folinic acid calcium salt to create the standard curve, including points: 0, 10, 20, 40, 60, 80, 100, 120fmol. We make the *L. casei* growth curve base on those points. There is a linear relationship between the growth of bacteria and folate level among the range from 0 to 120fmol. We can calculate folate concentration in the samples comparing with the standard curve. Also, we have to make sure the sample concentrations are in the range (0~ 120 fmol). Due to the bacteria activity status, there may be variation between each plate. So we have to set up standard curve in each plate.

To generate the standard, folinic acid calcium salt was used to make the highest concentration with sterile water, and then a 100X serial dilution was performed until the final concentration: 2fmol/µl as the working solution. The

storage solution is stored in -80ºC. Based on our data, a fresh standard needs to be made for each assay to get good slope of the standard curve.

Preparation of Conjugase Solution

Weigh 0.5g chicken pancreas conjugase (chicken pancreas powder lyophilized, Pel-Freez, Rogers, Arkansas) and put into 50.0mL beaker -covered with aluminum foil to block light. Add 30.0mL phosphate buffer pH 7.0 (0.69% w/v NaH_2PO_4-H_2O, 1.79% w/v Na_2HPO_4-$12H_2O$).   Mix for 15 minutes at room temperature. Transfer to 50.0mL volumetric flask, bring total volume with phosphate buffer pH 7.0 to 50.0mL - stir. Centrifuge at 5000 g for 10 min at 4°C. Store at -20°C.

Folate was removed from the conjugase to make sure there is no extra folate in the conjugase (Liu, Pickford et al. 2011). 250mg of activated charcoal were added to 5ml conjugase solution, mix well and incubate overnight at 4°C. Centrifuge at 12000rpm for 10min. The supernatant was removed, flash frozen, and stored at -80°C.

Statistical Analysis

Differences between folate adequate and folate depletion were analyzed by Student's *t*-test. A *p*-value of < 0.05 was considered significantly different. *P* values of < 0.05 and *P* values of < 0.01 are presented. Data are presented as means ± SEMs. All statistics were performed using Microsoft Excel.

RESULTS

The Lactic acid bacteria have no ability to synthesize the B vitamins but they have the transport ability of the B vitamins (Henderson, Suresh et al. 1986, Shane 2011). *Lactobacillus casei's* growth is promoted by the folate concentration, and this lactic acid bacteria has equal response to all folate monoglutamate forms (Snell and Peterson 1940). Since *L. casei* has such advantages, the researchers used this strain growth curve to detect the folate concentration. To generate folate standards for use in developing the microbiological folate assay, the serial dilution was made to get 2fmol/µl of folinic acid calcium as shown in the methods. During the setting up of the 96 well plate, the 0, 10, 20, 40, 60, 80, 100 & 120 fmol of the standard were added to the serial wells and triplicated to determine the linearity and the sensitivity of the microbiological assay. The results demonstrate the ability of the microbiological assay to detect different concentrations of folate standards and the linearity of this assay (Figure 3).

Folate is oxidizable and light sensitive. When we use the degraded folate standards, the *L. casei* growth curve is not sensitive to detect the distinct concentration of the folate standards. We found the growth of *L. casei* responded to 120 fmol frozen folate standard decreased ~ 53% than to 120 fmol fresh standard (Figure 4). So making fresh folate standards is most important for calculation of the sample's folate level.

Folate derivatives have different length of glutamate chains. *L. casei* didn't show different growth curve among the medium that contained monoglutamates,

or diglutamates or triglutamates(Shane 2011). *L. casei* still has the ability to transport the long-chain folylpolyglutamates with lower rates (Tamura, Shin et al. 1972, Shane and Stokstad 1976). The entire folate was monoglutamate form in plasma, but folylpolyglutamates form in the red blood cells or tissues. It is necessary to hydrolyze glutamate chain length for the quantification of total folate level by the *L.casei* assay. The researchers used the hog kidney (Shane 2011), rat plasma (Wani, Hamid et al. 2012), or chicken pancreas as the hydrolase which will hydrolyze the polyglutamate chain to monoglutamate. No one has compared these different conjugase efficiency, and also it is rare for a paper to show the efficiency of the conjugase. We compared the conjugase functions between the rat plasma and chicken pancreas powder. That's never been shown in other papers. Our results show the chicken pancreas conjugase has 30% more function than mouse plasma (Figure 5A). Also our data determine the optimal conjugase incubation time is 4 hours (Figure 5B).

To confirm our assay is optimized, we detected the effect of different amounts of dietary folate on mouse serum folate levels. Our assay detects significant differences in serum folate between the Folate adequate (FA) group and the Folate depletion (FD) group (Figure 6). We also determined one week is the optimal storage length for the frozen serum sample. When the serum was frozen for over 3 weeks, the differences between the FA and FD group disappeared (Figure 6). Also, we detected the folate level in different tissues of young mice. The folate level from high to lowest is: liver, kidney, testis, small

intestine, colon and brain. Our results are consistent with the literature (Varela-Moreiras and Selhub 1992) (Figure 7).

In addition to measuring the folate level in different mouse tissues, we also detected the folate level in two different kinds of mouse cell lines MEFs & BNL C2, which were grown in the media with/without the folate as described in methods. Our assay showed the folate level was completely depleted in the cells grown without the folate in the media (Figure 8). There is significant difference between the FA & FD groups. Our assay successfully confirms the condition of folate depletion that provides us an efficient model for the studies on the folate depletion.

CONCLUSION

Among all the methods to determine folate levels, the *L.casei* microbiological folate assay has been widely used as the gold standard because of simplicity of operation, economy of reagents, quickness, sensitivity to low amount of folate and clear results. In this study, we developed the assay for our lab. This assay has some adaptation to the microbiological assay described by Horne and Patterson (Horne and Patterson 1988). We determine the initial concentration of *L. casei*, which make it possible to have consistent results of the standard curve. We used the refresh bacteria culture instead of frozen strain, which make sure the bacteria growth ability is good. Furthermore, we used this assay to detect the intracellular folate levels and the tissue folate levels with the treatment of conjugase instead of determining the chemical folic acid level

described by Horne. These details about conjugase treatment have rarely been shown in other papers. And we compared the total folate levels among different mouse tissues by our assay and found the total folate distribution between tissues. The sequence from highest folate level to lowest is: liver, kidney, testis, small intestine, colon and brain. In addition, we found that the conjugase concentration, incubation time of conjugase and frozen time of samples could dramatically affect the accuracy of this assay. The optimal incubation time of conjugase is 4 hours and sample good frozen time is one week.

Folate, as an important nutrient, has a critical relationship with human health. Folate has important bio-functions during the one-carbon pathway and is involved in the conversation from dUMP to dTMP. There are evidences showing folate deficiency may induce the uracil misincorporation in DNA (Blount, Mack et al. 1997, Duthie 1999). And other evidence showed the folate depletion prevented the induction of BER pathway (Unnikrishnan, Prychitko et al. 2011) and the DNA strand break response to folate depletion increased hugely when the BER activity reduced ~50% (Cabelof, Raffoul et al. 2004). With the DNA damage/mutation, DNA strand break and BER ability imbalance, folate deficiency may affect the human health and have a relationship with human disease such as anemia and neural tube defects (Lanska 2010), and tumor/cancer. The ability to detect folate levels in serum and tissues gives us the ability to identify and prevent these human disease, also gives us the good methods to confirm the folate status when set up the research project on folate deficiency.

Table 1 Folate assay methods.

Folate assay methods	In vivo folate levels	Citation
Microbiological assay:		

Lactobacillus casei microbiological assay	Hepatic folate (nmol/g)
	
	Folate fed
	  17nmol/g (weanling)
	  17nmol/g (12 month old)
	
	Folate depleted
	  2.7nmol/g (weanling)
	  1.8nmol/g (12 month old)
		(Ghandour, Lin et al. 2002)

Lactobacillus casei microbiological assay	Plasma folate (umol/L)
	(young value, old value)
	
	  Folate deficient 1.5, 0.9
	  Folate replete 34.1, 30.6
	  Folate supplemented 53.9, 55.5
	
	Colon (nmol/g)
	(young value, old value)
	
	  Folate deficient 1.3, 0.7
	  Folate replete 4.7, 3.0
	  Folate supplemented 5.6, 4.4
		(Choi, Friso et al. 2003)

Lactobacillus casei microbiological assay	Serum folate (ng/ml):
	
	 Folate fed (2mg folate/kg diet)
	  39.0 (3 months)
	  35.4 (6 months)
	
	Folate depleted (0mg folate/kg diet)
	  12.1 (3 months)
	  10.8 (6 months)
	
	Folate supplemented (8mg folate/kg diet)
	  56.0 (3 months)
	  46.0 (6 months)
	
	Folate supplemented (20mg folate/kg diet)
	  49.9 (3 months)
	  43.3 (6 months)
		(Song, Medline et al. 2000)

Lactobacillus casei	Apc+/+ crossed to Shmt genotype as	(Macfarlane,

| microbiological assay | indicated (+/+, +/-, -/-)
Folate/choline fed (5 weeks)

Plasma (ng/ml)   58.56 (+/+)
                   58.34 (+/-)
                   40.82 (-/-)

Liver (fmol/ug pro) 51.80 (+/+)
                   56.65 (+/-)
                   50.77 (-/-)

Colon (fmol/ugpro) 35.14 (+/+)
                   21.46 (+/-)
                   17.09 (-/-)

Folate/choline depleted (5 weeks)

Plasma (ng/ml)   20.60 (+/+)
                   38.95 (+/-)
                    8.52 (-/-)

Liver (fmol/ug pro) 47.26 (+/+)
                   44.30 (+/-)
                   48.88 (-/-)

Colon (fmol/ugpro)   9.15 (+/+)
                   18.04 (+/-)
                   14.89 (-/-)
Apcmin/+ crossed to Shmt genotype indicated (+/+, +/-, -/-)

Folate/choline fed: (11 weeks)
 Plasma (ng/ml)   24.68 (+/+)
                   20.91 (+/-)
                   26.44 (+/-)

Liver (fmol/ug pro) 45.72 (+/+)
                   40.00 (+/-)
                   41.50 (-/-)

Folate/choline depleted: (11 weeks)
 Plasma (ng/ml)   11.79 (+/+)
                    8.37 (+/-)
                    9.97 (-/-) | Perry et al. 2011) |

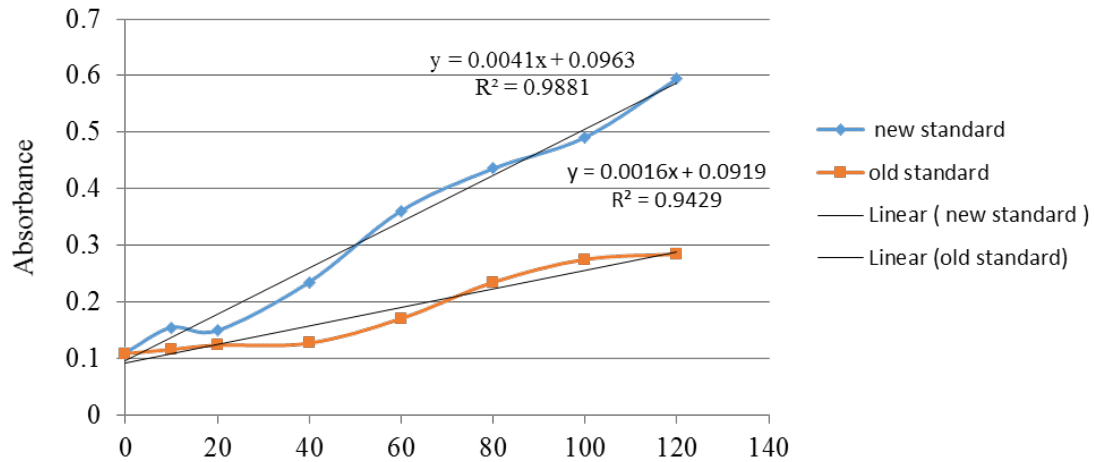|	Liver (fmol/ug pro) 28.49 (+/+) 23.25 (+/-) 29.44 (-/-)	
Lactobacillus casei microbiological assay	Folate/choline fed Plasma folate (ng/ml) 36.3 (wt) 46.8 (Tg) Liver folate (fmol/ug pro) 43.1 (wt) 51.3 (Tg) Folate/choline depleted Plasma folate (ng/ml) 7.4 (wt) 5.5 (Tg) Liver folate (fmol/ug pro) 36.1 (wt) 34.0 (Tg)	(MacFarlane, Anderson et al. 2011)
HPLC method:		
Combines of affinity chromatography and ion-pair HPLC	Folate levels (nmol/g) Folate fed: Liver 27.11 Kidney 11.69 Spleen 3.74 Brain 0.65 Folate depleted: Liver 11.10 Kidney 4.79 Spleen 1.29 Brain 0.60	(Varela-Moreiras and Selhub 1992)
HPLC	Whole blood folate Folate fed (supplemented)* 657000 ng/ml Folate depleted 125000 (no abx) 114000 (abx first 4 weeks) 61000 (abx last 4 weeks)	(Le Leu, Young et al. 2000)
Radioassay:		

Radioassay	Folate value in ng/mg protein
	
	Lymphocytes
	  Folate fed: 0.45
	  Folate depleted: 0.27
	
	Liver
	  Folate fed: 136.2
	  Folate depleted: 93.9
	
	Colon (descending)
	  Folate fed: 24.6
	  Folate depleted: 9.9
	
	Spleen
	  Folate fed: 16.5
	  Folate depleted: 7.9
	
	Kidney
	Folate fed: 58.6
	Folate depleted: 26.6
	
	Brain
	Folate fed: 20.4
	Folate depleted: 15.3
	
	Heart
	Folate fed: 9.2
	Folate depleted: 3.4
		(Duthie, Horgan et al. 2010)

Radioassay	Liver folate
	
	Folate fed
	  27.0µg/g
	
	Folate depleted
	  1.2 µg/g
		(Branda, O'Neill et al. 2007)

SimulTRAC-SNB radioassay kit	Serum folate Folate fed 60ng/ml Folate depleted <5ng/ml	(Cabelof, Raffoul et al. 2004)
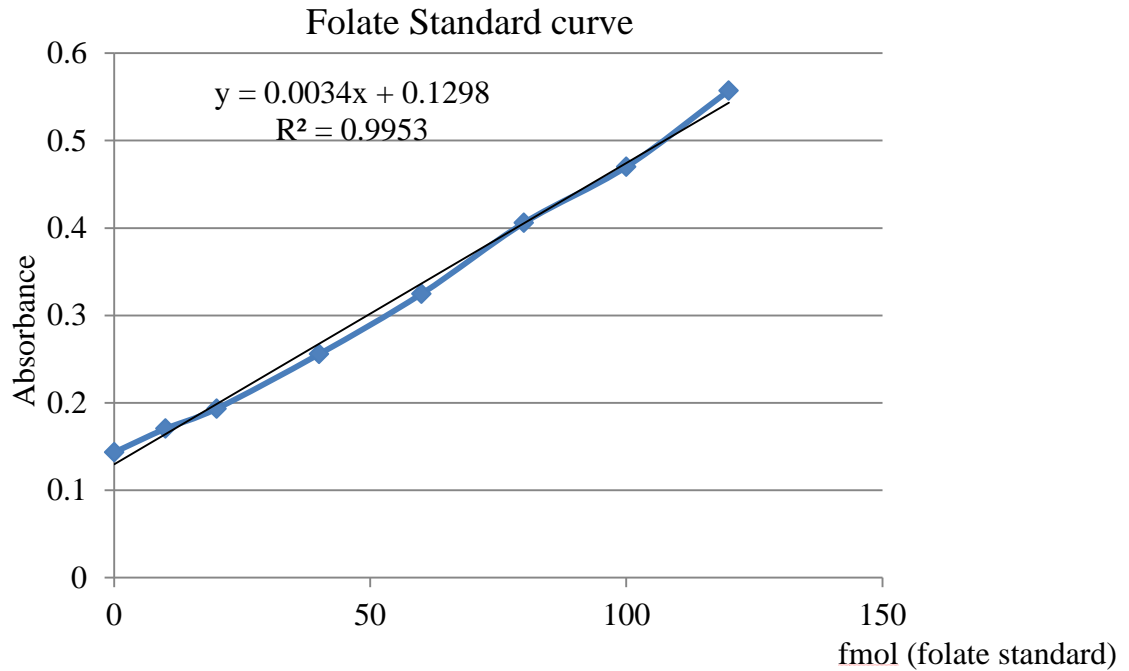
Figure 3: Folate standard curve. We used folinic acid calcium salt as the standard to detect the relationship between the folate concentration and *Lactobacillus casei* growth. During the setting up of the 96 well plate, the 0, 10, 20, 40, 60, 80, 100 & 120 fmol of the standard were added to the serial wells and triplicated to determine the linearity and the sensitivity of the microbiological assay. The results demonstrate the sensitivity and the linearity of this assay.

Fresh folate standard vs. frozen folate standard

$y = 0.0041x + 0.0963$
$R^2 = 0.9881$

$y = 0.0016x + 0.0919$
$R^2 = 0.9429$

- new standard
- old standard
- Linear (new standard)
- Linear (old standard)

Figure 4: Folate standard curve test. The fresh folate standard and frozen folate standard were used to make the standard curve through the *L. casei* assay. There are 8 points in the standard curve: 0, 10, 20, 40, 60, 80, 100, and 120 fmol. We found the growth of *L. casei* responded to 120 fmol frozen folate standard decreased ~ 53% than to 120 fmol fresh standard.
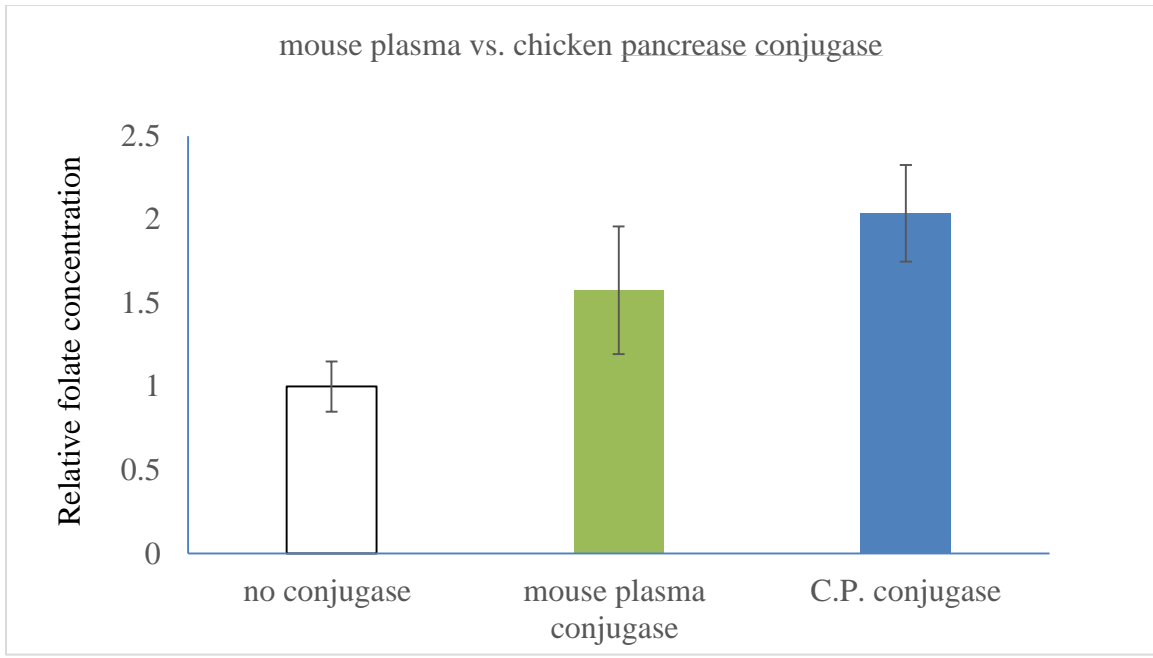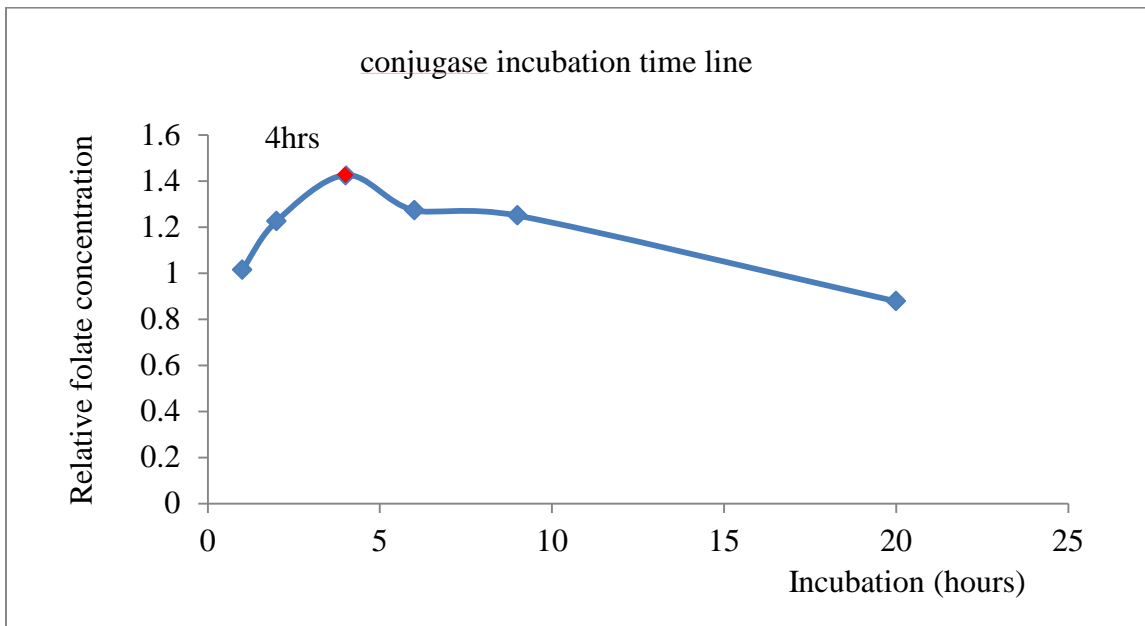
Figure 5A

Figure 5B

Figure 5: Conjugase test. *A*, Comparison of the conjugase functions between the mouse plasma and chicken pancreas powder. Our result shows the intracellular folate level treated by chicken pancreas conjugase has about 2fold higher than non-treated by conjugase. The intracellular folate level treated by mouse plasmas have about 1.6 fold than non-treated by conjugase. There is 30% more efficiency in chicken conjugase than mouse plasma. *B*, Also our data determines the optimal conjugase incubation time is 4 hours.
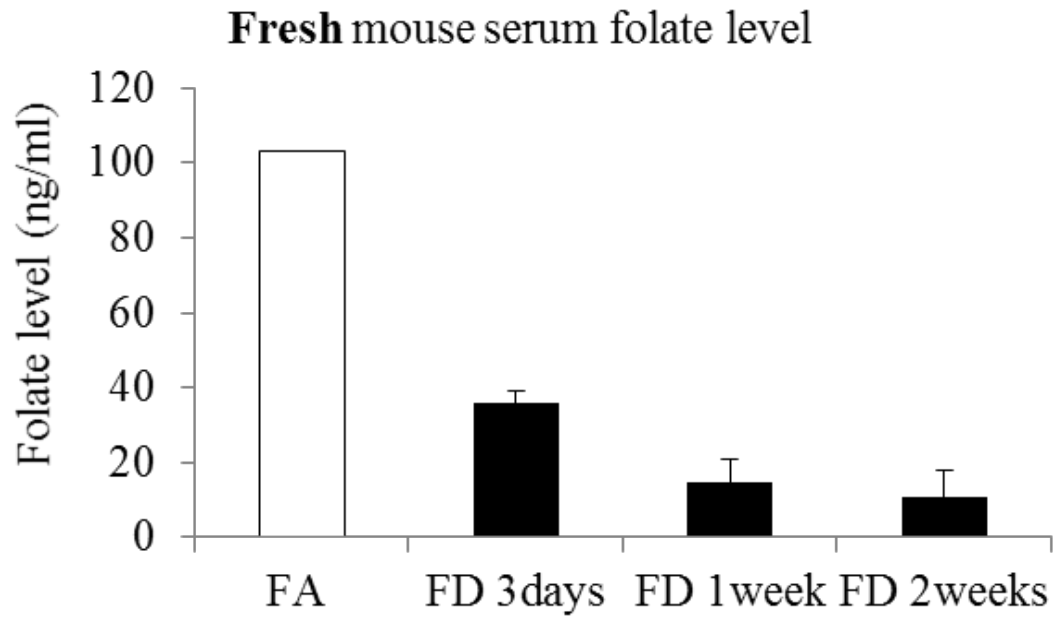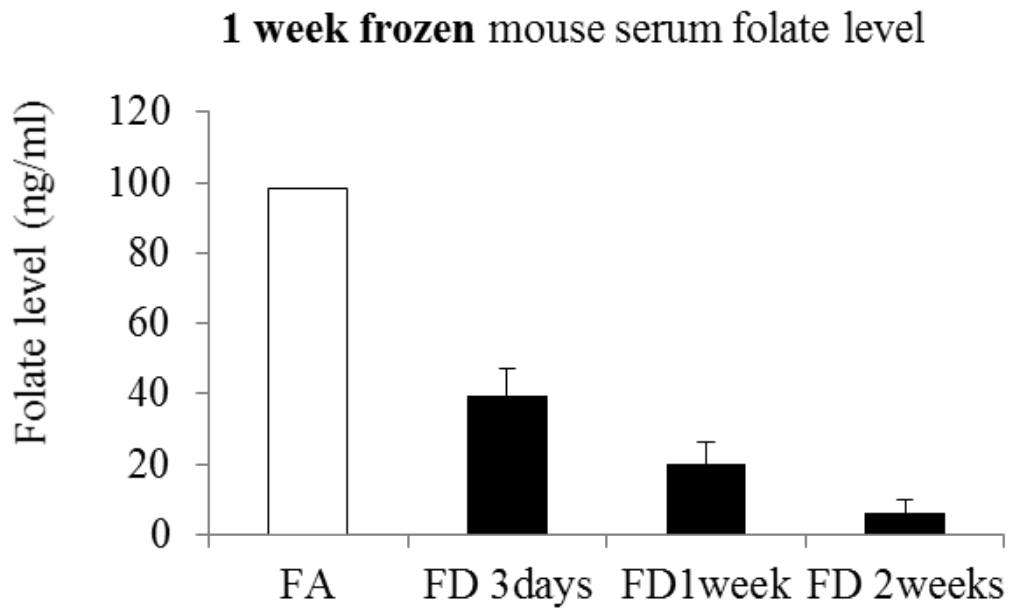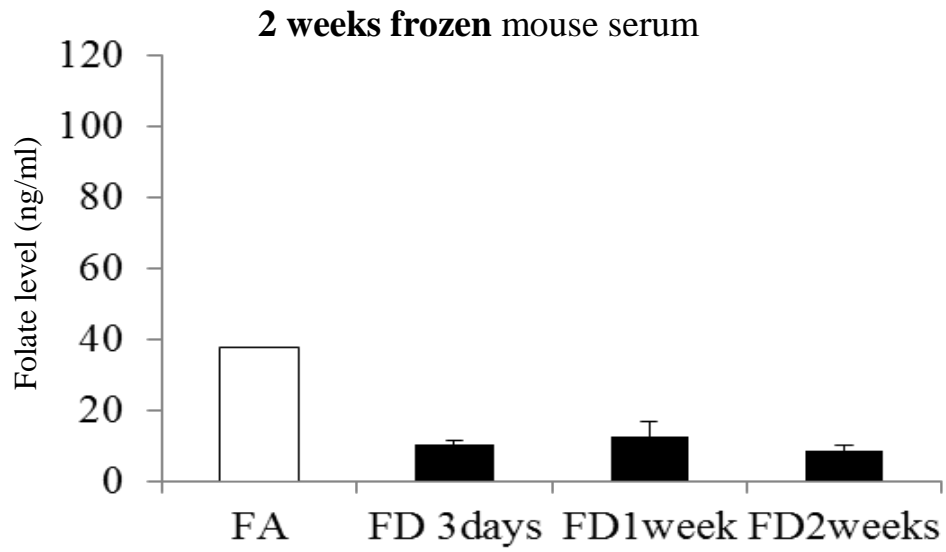
Figure 6A

Figure 6B

Figure 6C
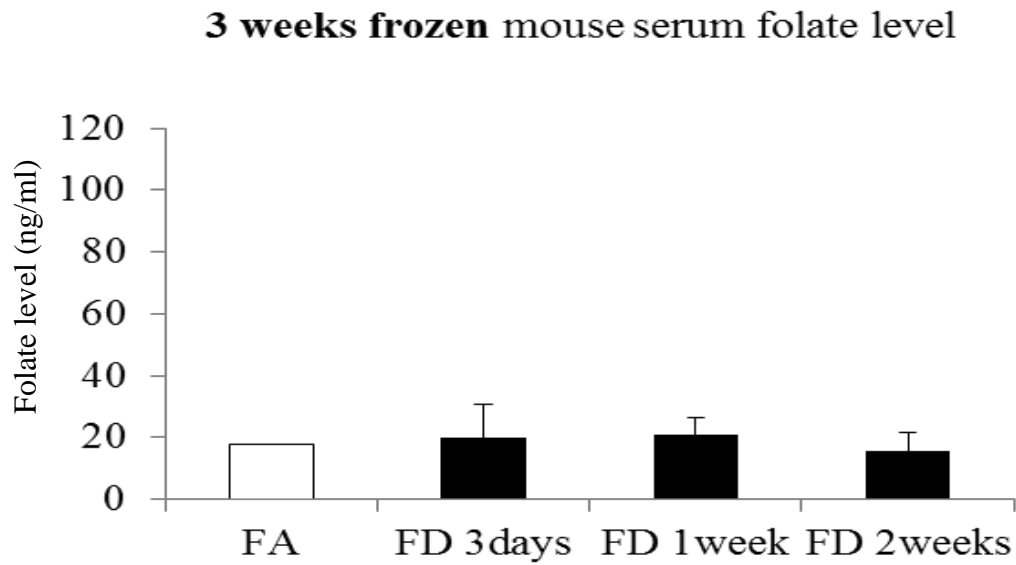
Figure 6D

Figure 6: Mouse serum folate level. We detected the mouse serum folate level of different group of diets with/without folate. *A*, to the fresh mouse serum folate levels, our assay could differentiate the significant differences between the Folate adequate (FA) group and the Folate depletion (FD) group. *B*, the mouse serum was frozen for one week, our assay still detected the significant difference between the FA and FD groups. *C*, the mouse serum was frozen for two weeks, all the groups folate levels decreased. The FA group folate level decreased about 60%. *D*, the mouse serum was frozen for three weeks, our assay couldn't detect the difference between FA and FD groups. The FA group folate level decreased about 80%. We found one week is the optimal storage length for the frozen serum sample. When the serum was frozen for over 3 weeks, the differences between the FA and FD group disappeared.
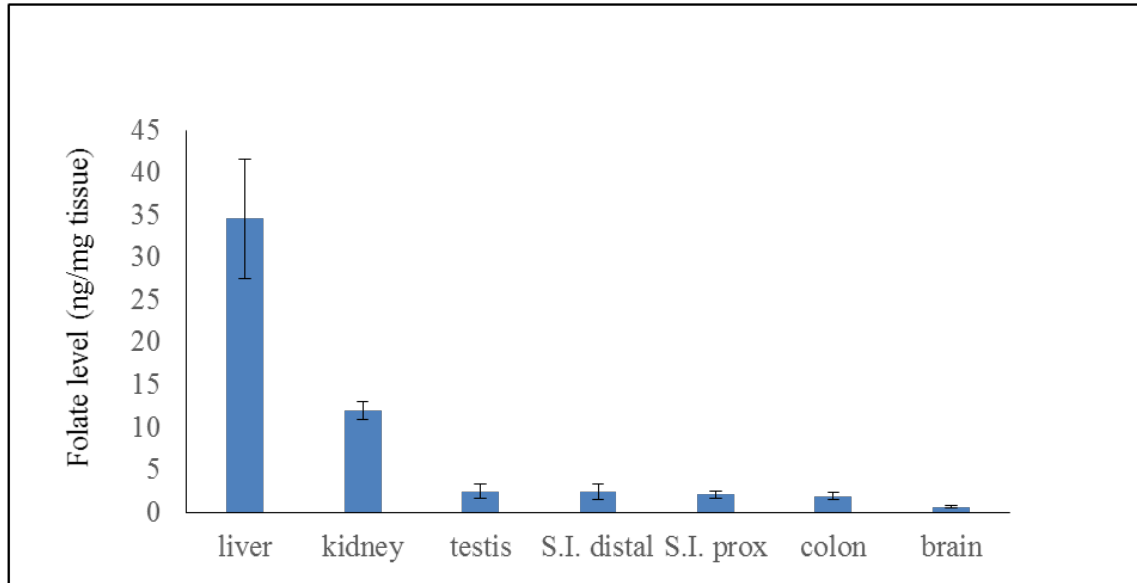
Figure 7: Folate level in different mice tissues. We detected the folate level in

different tissues of young mice. The folate level from high to lowest is: liver,

kidney, testis, small intestine, colon and brain.
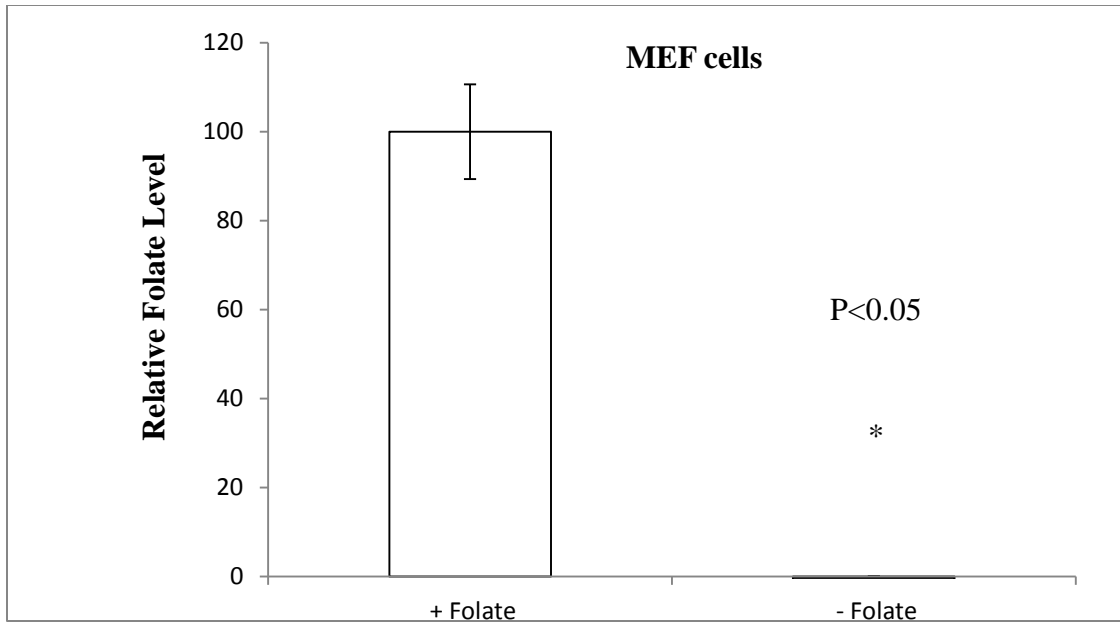
Figure 8A
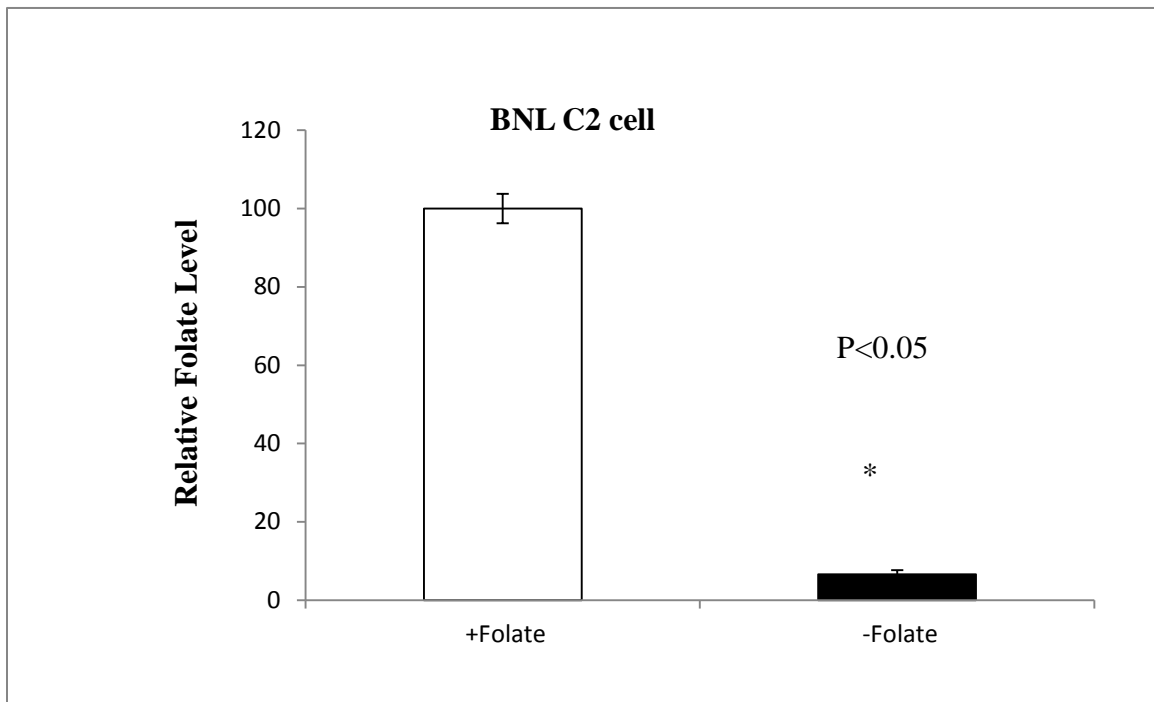
Figure 8B

Figure 8: Intracellular folate levels. Intracellular folate level were detected in two different kinds of mouse cell lines MEFs and BNL C2, which were grown in the media with/without the folate as described in methods**. *A*, MEFs cells folate level**. ***B*, BNLC2 cells folate level**. Our assay showed the folate level is completely depleted in the FD group. There is a significant difference between the FA & FD groups. FA, cells were grown in media with folate; FD, cells were grown in media without folate.

CHAPTER 3

DETERMINE THE IMPACT OF FOLATE DEPLETION ON URACIL ACCUMULATION IN DNA, DNA REPAIR CAPACITY, AND GENE EXPRESSION. DIRECTLY EVALUATE THE ROLE OF UDG ON URACIL ACCUMULATION.

As described in Chapter 1, folate deficiency limits one-carbon units, which inhibits the conversion from dUMP to dTMP. The uracil accumulation in DNA may happen. This Chapter focuses on the uracil accumulation in DNA response to folate depletion in cell. We choose MEFs (*UNG*$^{+/+}$), MEFs(*UNG*$^{-/-}$), BNLC2 cell lines as models. We detect the impact of folate deficiency on the UDG activity, BER (UDG initiated) activity, and the uracil level in DNA. This Chapter is trying to figure out the mechanism behind the uracil accumulation in DNA response to folate depletion.

METHODS

Tissue Culture/Folate depletion

The response to folate depletion was evaluated in two distinct cell types: SV-40 transformed mouse embryonic fibroblasts (MEFs; Tag 92) and BNL CL.2 cells, which are transformed liver cells derived from BALB/c mice (ATCC TIB-73TM). In addition, we evaluated the impact of *Ung* status on the response to folate depletion by comparing wild type (WT) MEFs to Ung-/- MEFs (Tag 207 and Tag 210; Endres et al., 2004). Cells were maintained in either folate-adequate or folate-free media with dialyzed serum. Initially, cells grown in folate-free media

were cultured in media supplemented with 10uM thymidine/60uM adenosine (T/A) to allow cell survival. Removal of folate from the media without T/A supplementation initially resulted in cell death. Stepwise reductions in the percent T/A was conducted over time, such that T/A concentrations were decreased every 3 passages until T/A supplementation was not required for survival. Cells were counted using TC10 Automated Cell Counter, (Biorad, Hercules, CA) and were seeded at identical densities.

Folate microbiological assay

Cells are harvested by trypsinization, centrifuged, washed with 1X PBS, flash frozen in liquid nitrogen and stored at -80° C for future analysis. Upon thawing, 20 volumes Buffer #1 (0.25M sucrose, 10mM HEPES, 10mM β–mercaptoethanol, 10Mm ascorbic acid) is added to the cell pellet which is homogenized to consistency. Homogenate is centrifuged at 12000 rpm for 30 min, supernatant is collected, and 0.2 volumes of Buffer #2 (10% w/v ascorbic acid, 1M β-mercaptoethanol, 0.25M HEPES, 0.25M CHES) is added to the supernatant. The cell lysate is boiled 5 minutes and centrifuged at 12000 rpm for 5 minutes. 100μl of supernatant is removed to a new tube with 80μl Buffer #1 and 20μl lyophilized chicken pancreas conjugase (Pel-Freez, Rogers, Arkansas). The conjugase mixture is incubated at 32°C for 4 hours, flash frozen in liquid nitrogen, and stored at -80°C. The lyophilized chicken pancreas conjugase is prepared as follows: 0.5 g lyophilized powder is added to 50mL phosphate buffer (pH 7.0), stirred at room temperature 15 minutes, and centrifuged at 5000 x g for

10 minutes at 4°C. Folate is removed from conjugase using activated charcoal as described by Ward et al (Liu, Pickford et al. 2011).

Intracellular folate level is measured using a 96-well plate *Lactobacillus casei* microbiological assay, modified from Home et al. (Horne and Patterson 1988). Briefly, *L. casei* is cultured overnight in growth media (4.7% w/v solution Folic Acid *Casei* Medium, DifcoTM, Becton Dickinson, Sparks, MD) supplemented with 0.025% w/v sodium ascorbate and 0.6µg/L folinic acid calcium salt (Santa Cruz, Santa Cruz, CA). The 300 µl reaction mixture contains 150µl media (9.4% solution Folic Acid Casei Medium, DifcoTMBecton Dickinson, Sparks, MD; 0.05% w/v sodium ascorbate), 8µl working buffer (0.16% w/v sodium ascorbate; 0.05mol/L potassium phosphate, pH 6.1), and cell lysate (1µl, 2µl and 10µl for each sample). A standard curve is created using folinic acid calcium salt over a range of 0 to 120 fmol, and is run on every plate. 20µl *L.casei* is diluted to OD=0.05. Multiple dilutions of lysate are used to ensure data fall within the standard curve. Sterile water is used to adjust final volume to 300µl. The light sensitive samples are covered and incubated at 37°C for 21hrs. Absorbance is read at 595nm using a Genios Basic TECAN-GENios plus plate reader and TECAN Magellan v6.00 software (Tecan Group Ltd., Zurich, Switzerland). Folate concentration was calculated by extrapolation from the standard curve. Folate concentration was considered significantly different from control at a *p*-value < 0.05.

Expression analyses

Total RNAs were isolated from cells (MEFs and BNL.C2) grown in full folate or folate free media using Isol-RNA Lysis Reagent per manufacturer protocol (5-Prime, Gaithersburg, MD). cDNAs were synthesized from 2μg RNA using random hexamer primers and an RT-PCR kit (Applied Biosystems, Waltham, MA), and purified with the QIAquick PCR Purification Kit (Qiagen, Valencia, CA). Real time PCR was conducted on a Light Cycler 480 machine (Roche, Indianapolis, IN). PCR reactions contained 2ug cDNA, 4mM $MgCl_2$, 0.4mM each of sense and antisense primers, and 2ml Fast Start DNA Master SYBR Green I enzyme-SYBR reaction mix (Roche). Primer sequences are detailed in Table 2. For all amplifications, PCR conditions consisted of an initial denaturing step of 99° C for 1min, followed by 35-50 cycles of 96° C for 10 s, 60° C for 10 s and 72° C for 5 s with a melting curve analysis from 40° C to 99° C to confirm specificity. External standards were prepared by cloning cDNA amplicons into TopoII vectors (Life Technologies, Carlsbad, CA), sequenced for confirmation, and used to create 10-log standard curves. All transcripts were normalized to either Rpl4 or Gapdh. Data are expressed as mean ± standard error of the mean (SEM) from at least three independent experiments, and is considered statistically significant at a *p*-value <0.05.

Isolation of Crude Nuclear Extract

Nuclear proteins for UDG activity assays were isolated using the Novagen NucBuster Protein Extraction Kit (EMD Chemicals, San Diego, CA. Cat.No. 71183-3). All samples and tubes were handled and chilled on ice, and all solutions were made fresh according to the manufacturer's protocol. The extract

was snap frozen in liquid nitrogen and stored at -80 °C. Crude nuclear extract was dialyzed against 1 liter of dialysis buffer (20 mMTris-HCl, pH 8.0,100 mMKCl, 10 mM NaS2O5, 0.1 mM DTT, 0.1 mM phenylmethylsulfonylfluoride, 1 µg/ml pepstatin A) for 4–6 h at 4 °C using Slide-A-Lyzer® mini-dialysis units suspended in a floatation device (Pierce). The dialyzed nuclear extracts were flash frozen in liquid nitrogen and stored at -80 °C. Protein concentrations of the nuclear extracts were determined according to Bradford using Protein Assay Kit I (Bio- Rad).

UDG Glycosylase Activity Assay

UDG activity was determined as previously described by Cabelof (Cabelof, 2004). Briefly, the 20µl reaction contained 70 mM Hepes (pH 7.5), 1 mM EDTA, 1 mM DTT, 75 mM NaCl, 0.5% bovine serum albumin, 90 fmol of 5'-end-labeled single-stranded uracil-containing oligonucleotide that was 3'-protected by an amino-spacer (5'-ATATACCGCGGUCGGCCGATCAAGCTTATT-3', MIDLAND, Midland, TX), and 5 µg of nuclear extract. Reactions were incubated at 37 °C for 1 h and then terminated by the addition of 5 µg of proteinase K and 1 µl of 10% SDS and incubation at 55 °C for 30 min. DNA was precipitated in glycogen, ammonium acetate, and ethanol at -20 °C overnight, re-suspended in a loading buffer containing 80% formamide, 10 mM EDTA, and 1 µg/ml each of bromophenol blue and xylene cyanol FF. Substrate and reaction products were separated on a 20% denaturing sequencing gel. Glycosylase activity (presence of an 11-mer band) was visualized and quantified using a Molecular Imager® System (Bio-

Rad) by calculating the relative amount of the 11-mer oligonucleotide product with the unreacted 30-mer substrate (product/product + substrate). The data are expressed as machine counts/µg of protein. Negative controls consisted of the reaction mixture and oligonucleotide in the absence of nuclear extract. 1unit of uracil DNA glycosylase inhibitor (New England Biolabs, Ipswich, MA) was added to one sample in each reaction to determine whether incision activity was the result of UDG specifically or another uracil-specific glycosylase.

Uracil initiated DNA base excision repair assay

The BER capacity was determined as described in a previous paper (Cabelof, Raffoul et al. 2004). Briefly, end-labeled and purified 30-bp oligonucleotides (upper strand, 5′-ATATACCGCGGUCGGCCGATCAAGCTTATT-3′; lower strand, 3′-TATATGGCGCCGGCCGGCTAGTTCGAATAA-5′) containing a G:U mismatch and an HpaII restriction site (CCGG) and protected by a 3′ amino spacer were incubated in a reaction mixture (100 mM Tris-HCl, pH 7.5, 5mM MgCl$_2$,1mM DTT, 0.1 mMEDTA, 2 mM ATP, 0.5 mM NAD, 20 µM dNTPs, 5 mM di-Tris-phosphocreatine, 10 units of creatine phosphokinase) with 50 µg of nuclear extract isolated from cells maintained in either folate-adequate or folate-free media with dialyzed serum. The reaction mixtures were incubated for 30 min at 37 °C, followed by 5 min at 95 °C to stop the reaction. The duplex oligonucleotides were allowed to reanneal for 1 h at room temperature and spun down to pellet the denatured proteins. The duplex oligonucleotides present in the supernatant were treated with 20 units of HpaII (Promega, Madison, WI) for 1 h

at 37 °C and separated by electrophoresis on a 20% denaturing sequencing gel. Repair activity (presence of a 14-mer band) is visualized and quantified using a Molecular Imager® System (Bio-Rad) by calculating the ratio of the 16-mer oligonucleotide product with the 30-mer substrate (product/substrate). The data are expressed as machine counts/μg of protein.

Uracil detection:

Uracil was detected as described by Cabelof et al. (Cabelof, Nakamura et al. 2006) and modified by Simon et al. (Simon, Ma et al. 2012). DNA was isolated from cell lysates using Qiagen (Valencia, CA) gravity tip columns per manufacturer's protocol. Briefly, 4 μg DNA was blocked for 2 h at 37° C in a tris/methoxyamine buffer (100 mM methoxyamine (Sigma–Aldrich, St Louis, MO) and 50 mMTris–HCl, pH 7.4). DNA was precipitated with 7.5% v/v 4 M NaCl and 4 volumes ice-cold 100% ethanol and re-suspended in TE buffer, pH 7.6. DNA was then treated with 0.4 units Uracil DNA Glycosylase (New England Biolabs, Ipswich, MA) for 15 min at 37° C, immediately precipitated and re-suspended in TE buffer, pH 7.6. DNA was then probed with 2 mM aldehydic reactive probe (Dojindo Molecular Technology, Rockville, MD) for 15 min at 37° C followed by ethanol precipitation and re-suspension in TE buffer. DNA was then heat denatured, immobilized onto a nitrocellulose membrane (Schleicher and Schuell Bioscience, Dassel, Germany), and baked under vacuum. The dried membrane was washed in 5X SSC for 15 min at 37° C, then incubated in a pre-hybridization buffer (20 mMTris, pH 7.5;0.1 M NaCl; 1 mM EDTA; 0.5% casein w/v; 0.25% BSA w/v; and 0.1% Tween-20 v/v for 30 min at room temperature). Streptavidin-

POD conjugate (Roche, Indianapolis, IN) was added at a 1:2000 dilution for 45 minutes at room temperature. Membrane was washed in TBS/Tween-20 three times at 37°C, incubated in ECL solution (Pierce-Thermo Fisher, Rockford, IL) for 5 min at room temperature, then visualized and quantified using a ChemiImagerTM system (BioRad, Hercules, CA). The concentration of DNA loaded on membrane was quantified using SYBR-Gold (Life Technologies, Carlsbad, CA), and data were normalized to DNA concentration. Data are expressed as the integrated density value per microgram of DNA loaded on the membrane.

Statistical Analysis

Differences between folate adequate and folate depletion were analyzed by Student's *t*-test. A *p*-value of < 0.05 was considered significantly different. *P* values of < 0.05 and *P* values of < 0.01 are presented. Data are presented as means ± SEMs. All statistics were performed using Microsoft Excel.

RESULTS

Experimental reduction in intracellular folate

The cells were grown in the media with folate present or absent. For the cell's survival without folate, we put Thymidine/Adenosine supplement and stepwise reduce the T/A supplement until the cells were able to survival without the supplement. We grew the cells in the folate adequate or folate deficiency condition for three passages and collected the cell pellets as described in the methods. Then we detected the intracellular folate level through the *Lactobacillus*

casei microbiological folate assay. Our data show the intracellular folate level were depleted through growing in the folate-free medial (Figure 9). Through this method we set up the folate depleted cell model. That makes it possible to connect our findings to the intracellular folate level.

Effect of folate depletion on doubling time and p21 gene expression

Folate carries and transfers one-carbon units during the DNA synthesis and DNA methylation. The folate may have impact on the production and maintenance of new cells. P21, protein cyclin-dependent kinase inhibitor (CKI), binds to and inhibits the activity of cyclin-CDK2, -CDK1, and –CDK4/6 complexes, and regulates the cell growth (Gartel and Radhakrishnan 2005). Also p21 is controlled by the tumor suppressor protein p53 and mediates the cell cycle G1 phase arrest in response to the stress stimulation (Rodriguez and Meuth 2006). We observed that folate deficiency results in the cell growing slowly. The cell doubling time increased in all the cell lines response to the folate depletion: 1.75fold in MEF ($UNG^{+/+}$), 3.82 fold in MEF ($UNG^{-/-}$), 3.03 fold in BNLC2 (Figure 10). Also we observed the cell doubling time increased 1.06 fold in MEFs when *UNG* knocked out under folate adequate condition (Figure 10). Folate status affects the cells' growth rate. Consistent, we observed the p21 gene expression level were highly induced by the folate deficiency: 8 fold in MEF ($UNG^{+/+}$), 18 fold in MEF ($UNG^{-/-}$), 4 fold in BNLC2 (Figure 11). Our observation suggests the stress of folate depletion has negative effect on the cell cycle. In the future we will determine the protein level of p21 and p53, and the cell cycle phase analysis

to confirm the folate deficiency slows the cell growth and arrests the cell in specific phases during the cell cycle.

Effect of folate depletion on uracil level in genomic DNA

Folate transfers one carbon units and converts the dUMP to dTMP; further, some research papers show the folate deficiency inducing the uracil accumulation in DNA (Blount, Mack et al. 1997, Duthie 1999, Kronenberg, Harms et al. 2008). However, we have not observed uracil accumulation in liver tissue of mice fed folate deficient diet (unpublished data, Cabelof and Heydari). Is the uracil level in genomic DNA response to folate depletion tissue/cell specific? With this question, we determine the uracil level in two cell lines (Figure 12): mouse embryonic fibroblasts MEF ($UNG^{+/+}$), BNLC2 mouse liver cells. There are two opposite results. In MEFs, 30% more uracil accumulated in DNA in response to folate depletion; but in BNLC2 cells, uracil does not accumulate under folate depletion condition. It brings us strong motivation to discover the mechanism behind the different phenotype.

Effect of folate depletion on UDG activity and UDG initialed BER activity

Folate transfers the one-carbon unit and has an important role during thymidine synthesis through the conversion from dUMP to dTMP. Folate depletion results in limiting one-carbon units and affects the thymidine synthesis through the pathway from dUMP, which changes the nucleotide pool for DNA synthesis. Misincorporated uracil in DNA should be removed by UDG initiated DNA base excision repair. The uracil present in DNA is the outcome of misincorporated uracil or cytosine deamination and uracil removal by DNA BER

repair. Since we observed two opposite outcomes from the two cell lines, MEFs and BNLC2, we hypothesize the UDG initiated BER ability to remove the uracil is different between the two different cell lines. We determined the UDG activity assay as described in methods (Figure 13). We used the nuclear protein collected from the cells to repair the oligonucleotide fragment with uracil misincorporated. As we expected, in response to folate depletion, UDG activity in MEF ($UNG^{+/+}$) is down-regulated about 40%, $p < 0.05$, but in the BNLC2 cells, this activity is up-regulated about 2 fold, $p < 0.05$ (Figure 14). Up regulation of UDG removes uracil in DNA, which results in no uracil accumulation secondary to folate depletion in BNLC2 cells. And the down-regulated ability to remove uracil in MEFs explains uracil persistence in DNA. To confirm our hypothesis, furthermore, we detect the UDG initiated BER activity using the same nuclear protein extracts. The results were consistent with the UDG activity, BER activity is down-regulated about 50% ($p < 0.01$) in MEFs, and up-regulated about 50% ($p < 0.01$) in BNL C2 cells (Figure 15). The BER activity is different between the two cell lines; what about the gene expression level of the other enzymes involved in the BER pathway response to the folate status? So, we quantified the key BER enzyme transcript levels: Pol-β, Ape1, Xrcc1, and Ligase III. The results show in the BNLC2, response to the folate depletion, the UNG gene expression up-regulated to about 5 fold and all the other enzymes up-regulated too (Figure 16). Even in MEF ($UNG^{+/+}$), Pol-β, Xrcc1, and Ligase III up-regulated response to folate depletion, but the initial step enzyme UNG is not up-regulated (Figure 17). Smug1 is believed to have backup function of UNG, but in our study,

we did quantify the four major uracil DNA glycosylases transcripts: Ung, Tdg, Mbd4, Smug1. In MEFs cells, even the Smug1 and Mbd4 increased the transcript levels, but the initial removal of uracil activity is still down-regulated and the BER activity is still down-regulated. Smug1 and Mbd4 didn't show efficient backup function to Ung in MEFs. The Ung has the critical role during the uracil removal in MEFs.

Effect of UDG knockout on uracil accumulation

Does up-regulation of UNG increase the uracil removal and prevent the uracil accumulation in DNA? To get more direct evidence, we utilized the UNG knock out MEFs. First to confirm the UNG knock out, we quantified the transcript level and found that there is no gene expression of UNG, most the key BER enzymes (Tdg, Mbd4, Smug1, Pol-β, Xrcc1, and Ligase III) are up regulated, $p < 0.01$ (Figure 18). Then we observe the UDG activity and UDG initiated BER activity is completely abrogated in the MEFs($UNG^{-/-}$) cells (Figure 19). As the outcome, we observed 2.5 fold ($p < 0.01$) increase in uracil accumulation in the UNG knock out MEFs in response to folate depletion (Figure 20). Those observations further confirm our hypothesis, that UDG plays the key role during the uracil response to the folate depletion. When UDG activity increases, UDG initiated BER activity increases, and the ability to remove the uracil increases, and the outcome is no uracil accumulated in DNA as described in Figure 21.

Effect of folate depletion on folate metabolism genes expression

Folate transfers one carbon units to convert dUMP to dTMP with the catalyzation of thymidylate synthase as shown in Figure 1. Thymidylate synthase

(Ts) is the only gene essential for thymidylate biosynthesis (MacFarlane, Anderson et al. 2011). So, does the up-regulation of TS promote the thymidylate biosynthesis and prevent the uracil accumulation response to the folate depletion? We quantified genes involved in folate metabolism. We observed the cystathionine-β-synthase (Cbs), Gamma-glutamyl hydrolase (Ggh), methionine synthase (Mtr), thymidylate synthetase (Ts), dihydrofolate reductase (Dhfr), serine hydroxymethyltransferase (Shmt1) genes transcripts up-regulated response to the folate depletion (Figure 22). We explained that under the limitation of folate, the cells try to increase the synthesis of thymidylate through Dhfr, Shmt1, and Ts, increase the recycling from homocysteine to methionine through Mtr; and increase the homocysteine to cysteine through Cbs. MEFs and BNLC2 cell have the same phenotype as above, so it is not the reason for the different observation of uracil level in DNA. That further confirms our hypothesis, as to the uracil accumulation in DNA, the Udg initiated BER has an important role, and up-regulation of UDG is required for the prevention of uracil accumulation in DNA.

DISCUSSION

Folate is essential for genome integrity. Previous studies have shown that folate prevents genomic damage in human lymphocytes *in vitro*; the frequencies of micronuclei, nucleoplasmic bridges, nuclear buds in the binucleated cell were diminished when folic acid concentration was not less than 120 nmol/l (Lu, Ni et al. 2012). And folate deficiency may induce dysfunctional long and short telomeres (Bull, Mayrhofer et al. 2014). As Fenech reviewed, both *in vitro* and *in*

vivo studies with human cells, folate deficiency causes expression of chromosomal fragile sites, chromosome breaks, excessive uracil in DNA, micronuclei formation, DNA hypomethylation and mitochondrial DNA deletions et al. (Fenech 2012). Folate carries and transfers one-carbon units during DNA synthesis and DNA methylation. With folate deficiency, limited methyl group impact conversion from dUMP to dTMP, resulting in excess uracil being misincorporated in DNA. UDG initiated BER will start to remove the uracil. Under folate deficient conditions, the response is not universal across tissues or cells. With down regulation of UDG and BER (UDG initiated), uracil accumulates in DNA of MEFs, which will lead to mutation of A:T. When UDG activity is up-regulated with completion of BER, uracil will be removed and the genome keeps integrity. But up-regulated UDG without BER completion will result in no uracil accumulation in DNA, but the DNA strands break, as in liver tissue (Cabelof, Raffoul et al. 2004). Those will lead to genomic instability. (Figure 23). Since we found that tissues/cells respond to folate deficiency differently, and the uracil/folate pathway is a frequent target for chemotherapeutics, it may be important to choose the specific folate antagonist therapies toward different tissues.

Table 2

Quantitative real time RT-PCR primer sequences.

Gene	Sense primer 5' - 3'	Anti-sense primer 5' - 3'
Ung	ttcgggaagccgtacttcg	catctgggtccatgtaacac
Tdg	aagttcctaacatggcagtcac	atttcttcgacgtagcaggttt
Mbd4	cagcccacaaggattgaagt	ggaagtcagagctgccaaac
Smug	cactggggcctacccatga	ctcccaagcataatccaccg
Ogg1	tgctggcagatcaagtatgg	ctgtgccaggctgacatcta
B-pol (exon 12-13)	agcgagaaggatggaaaggaa	cgtgcgctctcatgttcttat
Ape1	acggggaagaacccaagtc	ggtgaggttttctgatctggag
Xrcc1	gctgggaccgtgttaaaattgt	acgtcttgttgatacgactgaag
Ligase3	tgcctgaaaaaggtactgttgg	atgccacaaagtagcgtttga
p21	cctggtgatgtccgacctg	ccatgagcgcatcgcaatc
Cbs	ccaggcacctgtggtcaac	ggtctcgtgattggatctgct
Ggh	ccataaggcccgatcttagtga	tctgttaggttagcacctcctc
Mtr	atccagcggtacaaactaagtg	catccggtaggccaagtgttc
Ts	aagggtgttttggaggagttg	ttggcatcccagattctcact
Fpgs	acaccctgcaaaccaatgc	ctccgtgccaggtacatctc
Dhfr	cgctcaggaacgagttcaagt	tgccaattccggttgttcaata
Shmt1	gggtcggattagagctgattg	ggtcccgccataatacctttg
Housekeeping genes		
Gapdh	aggtcggtgtgaacggatttg	tgtagaccatgtagttgaggtca
Rpl4	ccgtcccctcatatcggtgta	gcatagggctgtctgttgtttt

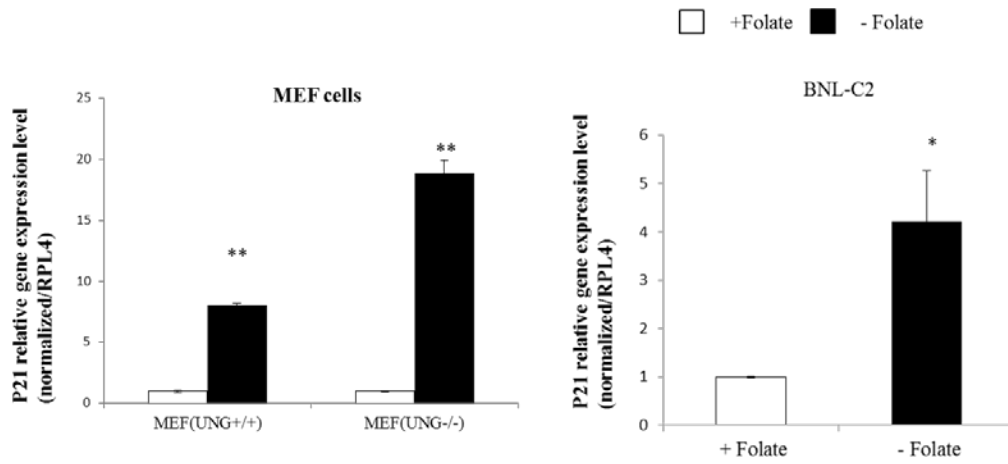## Effect of folate depletion on intracellular folate levels
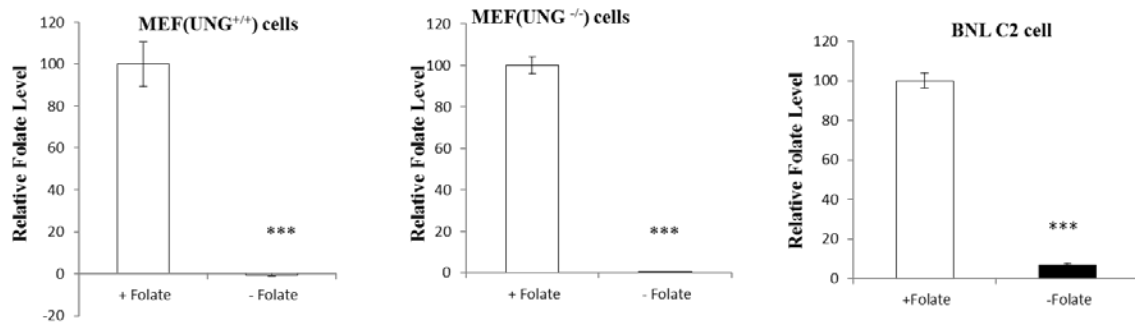
Figure 9: Cells grown in the absence of folate have severely depleted intracellular folate levels. A. MEF(*UNG*$^{+/+}$) cells; B. MEF(*UNG*$^{-/-}$) cells; C. BNL CL.2 cells. The cells were grown in the presence or absence of folate. Intracellular folate levels were determined using the *L. casei* microbiological assay described in Methods. Folate levels are calculated as described in methods and presented as a relative value, with + folate group set at 100. Data are expressed as mean ± SEM. There are 4 samples in each group. + folate, 4mg/L folic acid in media; - folate, no folate in media. ***p<0.0001.

Effect of folate depletion on doubling time
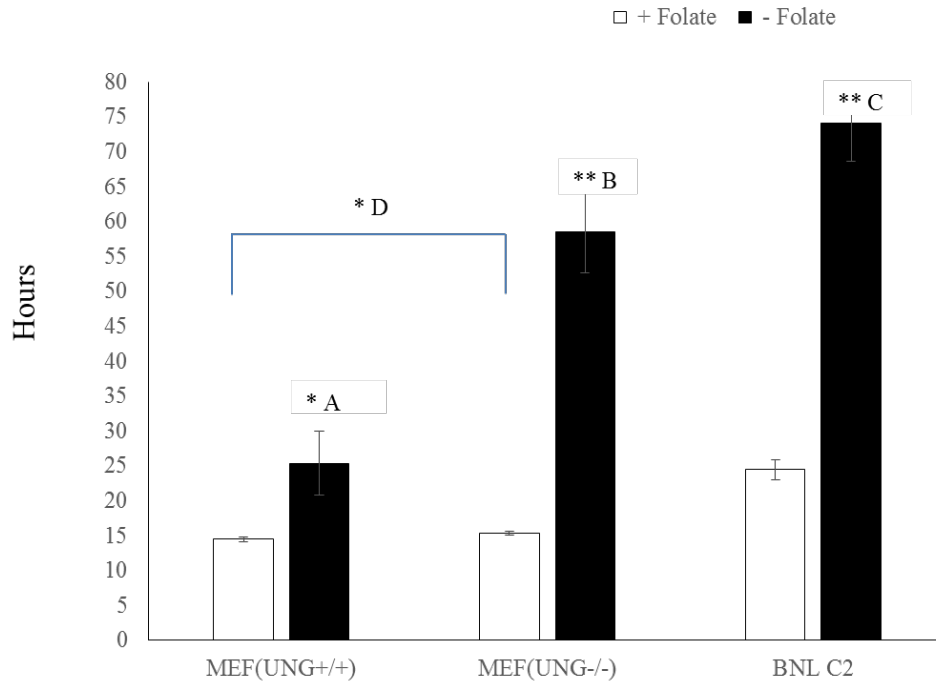
Figure 10: Folate depletion increases doubling time. Open bar has folate (4mg/L folic acid) in media; filled bar has no folate in media. A p value shows significant difference between groups, * $p<0.05$, ** $p<0.01$. **A. MEF(*UNG*^{+/+}) cells; B. MEF(*UNG* ^{-/-}); C. BNL C2 cells. D. In folate-adequate media, MEF(*UNG*^{+/+}) cells vs. MEF(*UNG* ^{-/-}).**

P21 gene expression

Figure 11: **The expression of p21 is up-regulated upon folate depletion in the cells**. Open bar has folate (4mg/L folic acid) in media; filled bar has no folate in media. **p<0.01, *p<0.05.
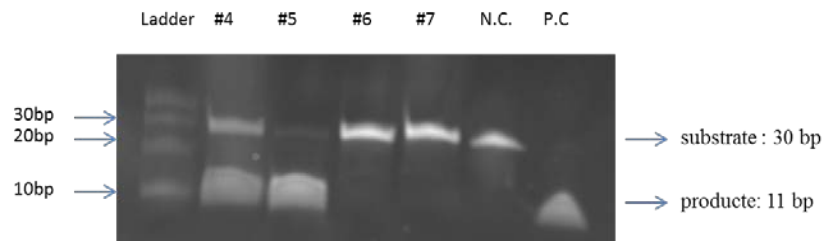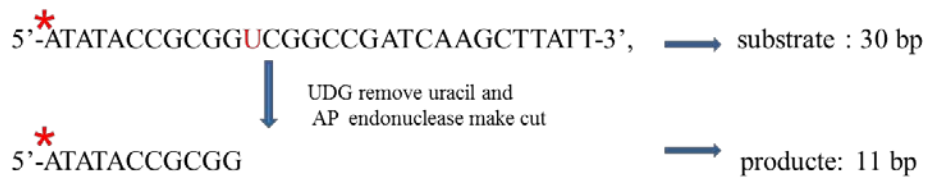
Effect of folate depletion on uracil accumulation
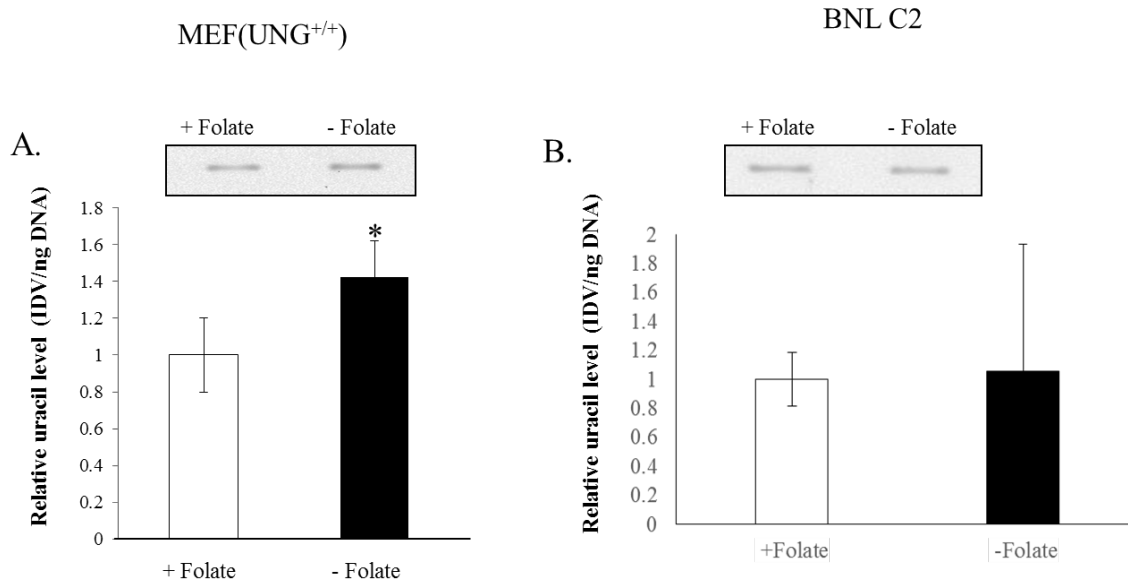
Figure 12: **Uracil accumulation in response to folate depletion.** A. MEF cells grown in the presence or absence of folate. B. BNL C2 cells grown in the presence or absence of folate. Genomic DNA was isolated and analyzed for uracil content as described in Methods. Integrated density volume (IDV) value was normalized to DNA concentration. Data are expressed as mean ± SEM. + folate, 4mg/L folic acid in media; - folate, no folate in media. $p < 0.05$. Image is representative image of data from triplicate experiments.

UDG activity assay
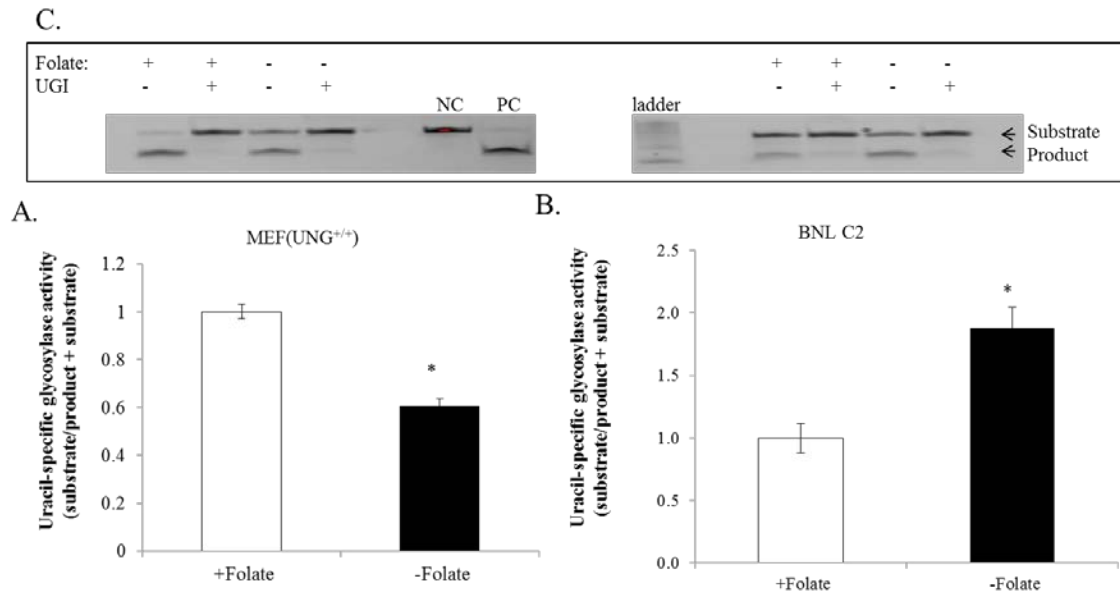
- Substrate: Single-strand uracil-containing oligonucleotide
  - 5'-end-fluorescein labeled
  - 3'-protected by an amino-spacer

*
5'-ATATACCGCGGUCGGCCGATCAAGCTTATT-3', ⟶ substrate : 30 bp

↓ UDG remove uracil and
   AP endonuclease make cut

*
5'-ATATACCGCGG ⟶ producte: 11 bp

N.C.: negative control.
P.C.: positive control.

Figure 13

Figure 14: Uracil-specific glycosylase activity in response to folate depletion. A. MEF cells grown in the presence or absence of folate. B. BNL C2 cells grown in the presence or absence of folate. C. Images of UDG activity. Glycosylase activity was quantitated as described in Methods. N.C.= negative control. P.C. = positive control. Ladder = 10bp ladder. UGI = Uracil DNA glycosylase inhibitor. Data is expressed as mean ± SEM. + folate, 4mg/L folic acid in media; - folate, no folate in media. *p<0.05. Substrate: 30base mer. Product: 11base mer. Image is representative image of replicate experiments. Data from MEFs displayed over MEF graph; data from BNL C2 cells displayed over BNL C2 graph.

Effect of folate depletion on UDG initiated BER activity
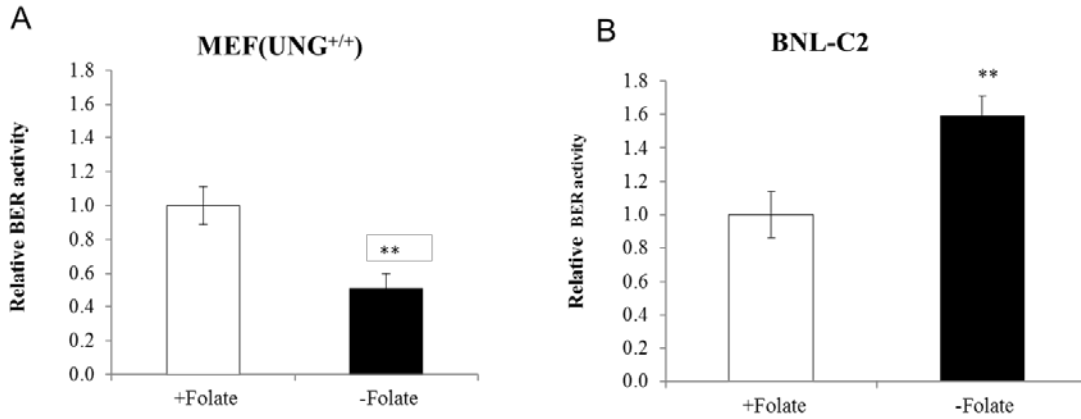
Figure 15: Effect of folate depletion on UDG initiated BER activity. A. MEF cells grown in the presence or absence of folate. B. BNL C2 cells grown in the presence or absence of folate. UDG initiated BER activity was quantitated as described in Methods. Data are expressed as mean ± SEM. + folate, 4mg/L folic acid in media; - folate, no folate in media. **$p<0.01$. Image is representative image of replicate experiments.
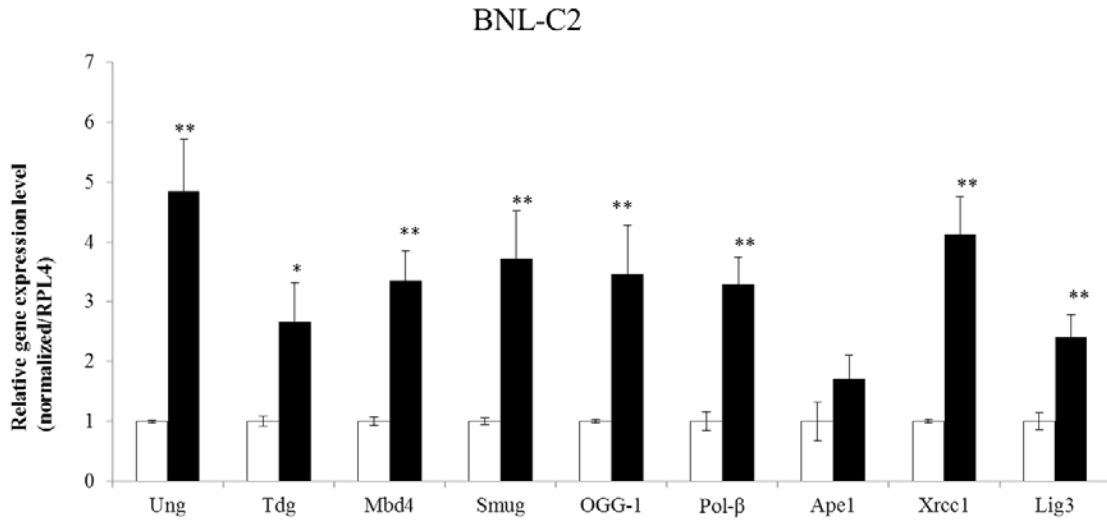
Figure 16: Base excision repair gene expression in BNL-C2 mouse liver cells in response to folate depletion. BNL-C2 mouse liver cells were grown in the presence or absence of folate and relative transcript abundance was determined as described in Methods. White bars = folate added; Black bars = folate depleted; *p<0.05; **p<0.01
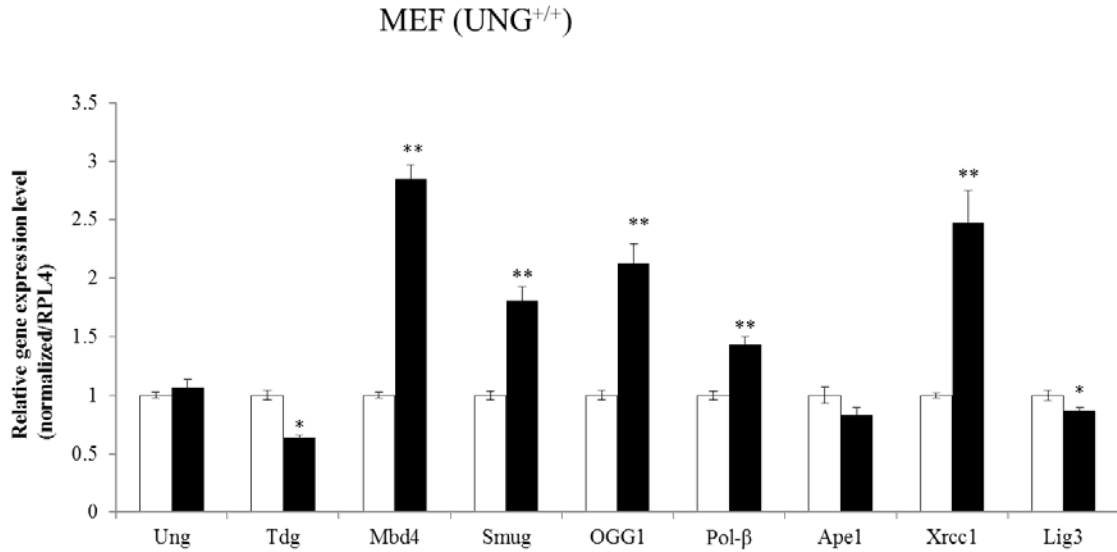
MEF (UNG$^{+/+}$)

Figure 17: **Base excision repair gene expression in MEF *Ung*-wildtype cells in response to folate depletion.** Mouse embryonic fibroblasts were grown in the presence or absence of folate and relative transcript abundance was determined as described in Methods. White bars = folate added; Black bars = folate depleted; *p<0.05; **p<0.01.
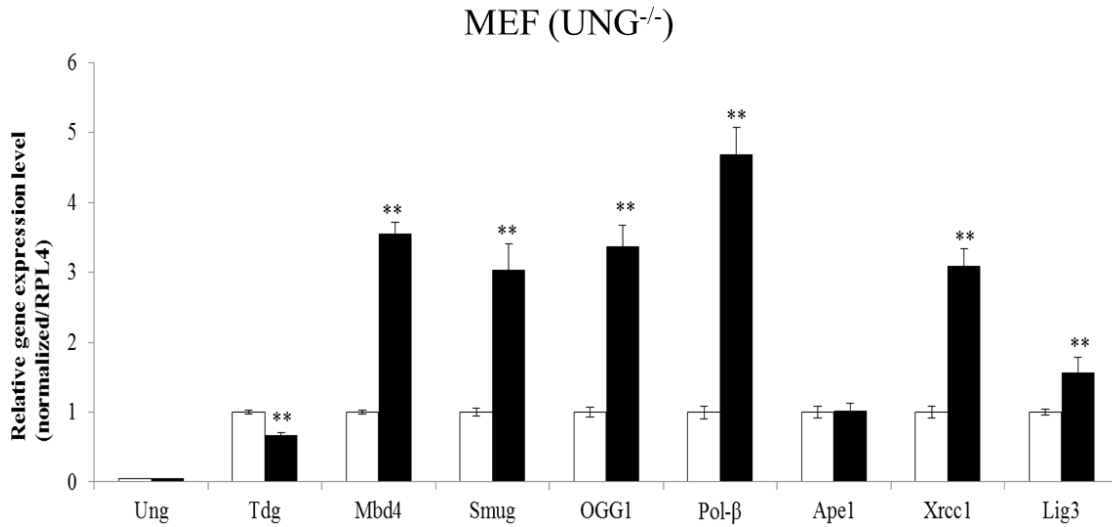
MEF (UNG$^{-/-}$)

Figure 18: Base excision repair gene expression in MEF Ung-null cells in response to folate depletion. Mouse embryonic fibroblasts (Ung-null) were grown in the presence or absence of folate and relative transcript abundance was determined as described in Methods. White bars = folate added; Black bars = folate depleted; *p<0.05; **p<0.01.
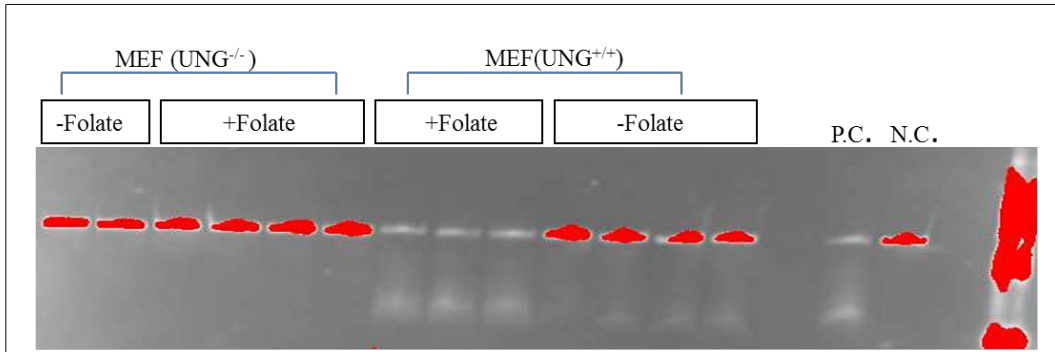
The UDG activity and UDG initiated BER activity is completely abrogated in the MEFs(UNG $^{-/-}$) cells

A. UDG Activity

B. BER Activity
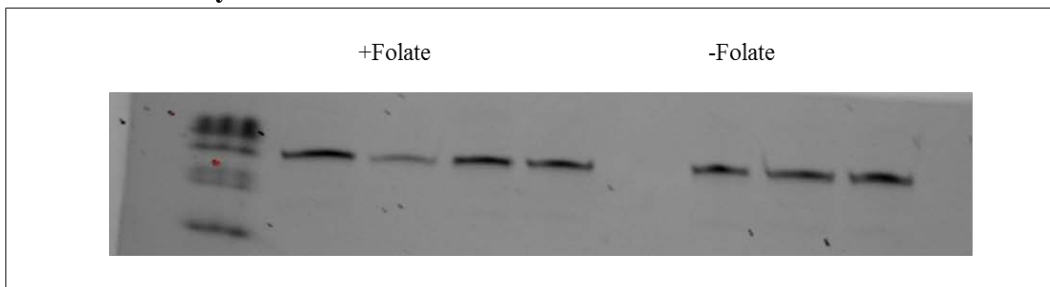
Figure 19: The UDG activity and UDG initialed BER activity is completed abrogated in MEFs(*UNG* $^{-/-}$) cells. A. UDG activity. B. UDG initiated BER activity. MEFs(*UNG*$^{-/-}$) cells were grown in the presence or absence of folate. N.C.= negative control. P.C. = positive control. Ladder = 10bp ladder. + Folate, 4mg/L folic acid in media; - Folate, no folate in media.

Effect of UNG knock out on Uracil accumulation response to the folate depletion
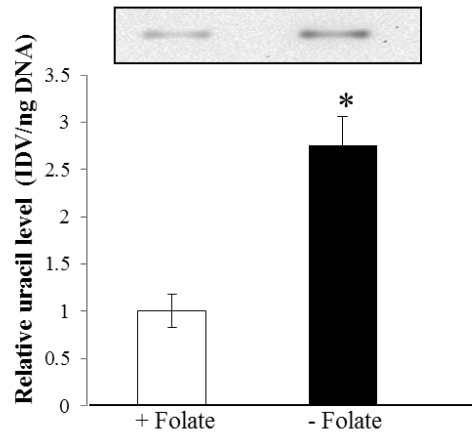
Figure 20: Absence of Ung magnifies folate-dependent accumulation of uracil in MEFs. Ung$^{-/-}$ MEF cells grown in the presence or absence of folate were evaluated for uracil accumulation. Genomic DNA was isolated and analyzed for uracil content as described in Methods. Integrated density volume (IDV) value was normalized to DNA concentration. Data are expressed as mean ± SEM. + folate, 4mg/L folic acid in media; - folate, no folate in media. **p<0.01. Image is representative image of data from triplicate experiments.

Response to Folate depletion
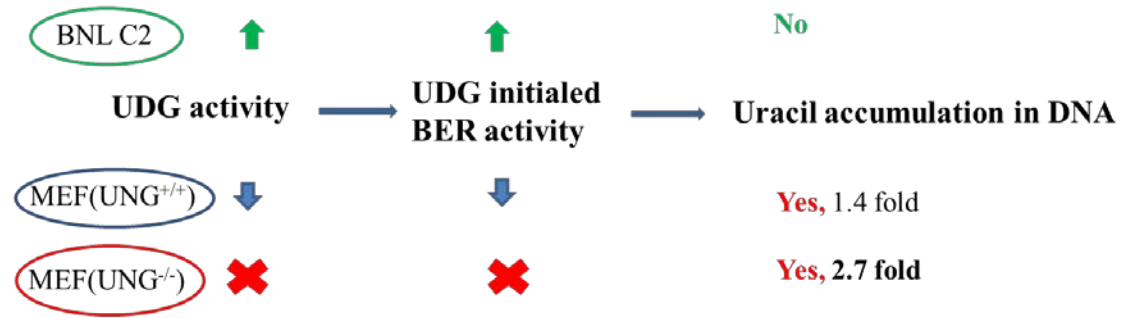
Figure 21
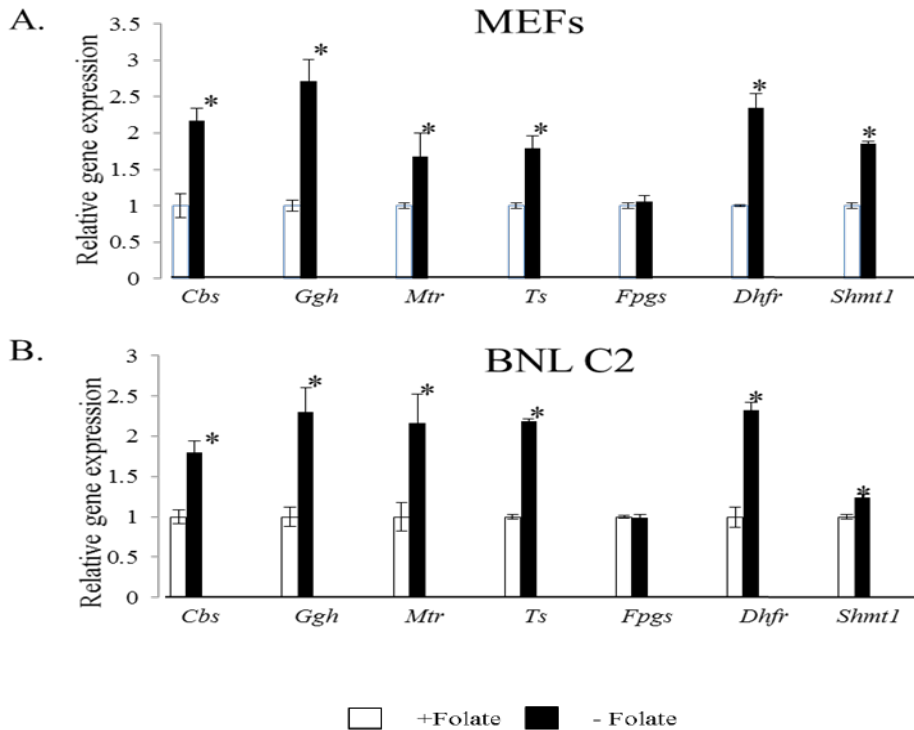
Figure 22: Relative transcript abundance of folate metabolizing enzymes in response to folate depletion is similar across cell lines. A. MEF cells grown in the presence or absence of folate. B. BNL CL.2 cells grown in the presence or absence of folate. Gene expression was quantified as described in Methods. Values for control group (+ folate) are set equal to 1.0, and experimental group (-folate) is expressed relative to control group. Data normalized to Rpl4 expression. White bars = folate added; Black bars = folate depleted; *$p < 0.05$. Cbs, cystathionine beta synthase; Ggh, gamma glutamyl hydrolase; Mtr, methionine reductase; Ts, thymidylate synthase; Fpgs, folypolylglutamate synthase; Dhfr, dihydrofolate reductase; Shmt1, serine hydroxymethyl transferase 1.

Genome instability, uracil accumulation and BER

- Folate depletion ⟶ methyl group limited

Uracil ⟶ Thymidine

Uracil misincorporation in DNA

UDG activity ↓
UDG initiated BER activity ↓

Uracil accumulation in DNA

UDG activity ↑
UDG initiated BER activity ↑

mutation

Uracil is removed ⟶ BER DNA repair complete

uncompleted DNA repair

strand break ⟶ chromosome damage ⟶ human diseases
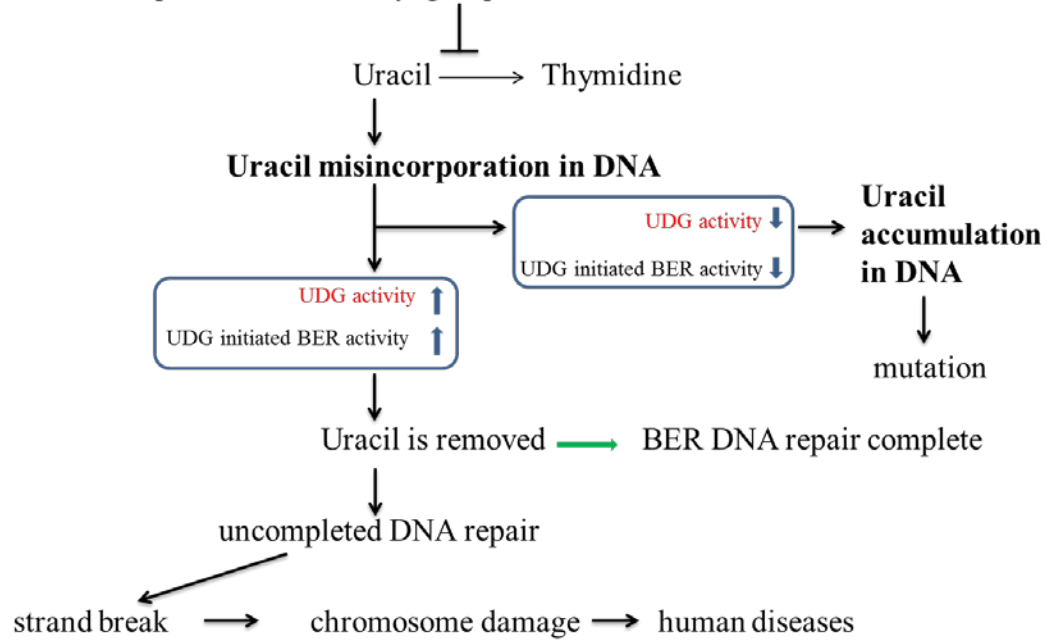
Figure 23

CHAPTER 4

THE IMPACT OF AGING ON FOLATE AND URACIL LEVELS IN MOUSE COLON TISSUE

We talk about the relationship among folate deficiency, uracil accumulation and aging in Chapter 1. With aging, there is reported to be folate reduction (Herrmann, Quast et al. 1999, Choi, Friso et al. 2003) and uracil accumulation in DNA (Simon, Ma et al. 2012). Under folate deficiency, there is also uracil accumulation in DNA (Blount, Mack et al. 1997, Duthie 1999). Our hypothesis is how the uracil accumulated in DNA response to the folate deficiency may be the mechanism by which uracil accumulates with aging. In Chapter 3, we provide evidence that up-regulation of UDG activity prevents uracil accumulation in response to folate depletion. Chapter 4 is focus on the impact of aging on the folate status and uracil accumulation in DNA.

METHODS

Animals

In an initial study, experiments were performed in young (4–6 months) and old (24–28 months) male specific pathogen-free C57BL/6 mice in accordance with the NIH guidelines for the use and care of laboratory animals. The animal protocol was approved by the Wayne State University Animal Investigation Committee. Mice were maintained on a 12-h light/dark cycle and were fed a standard mouse lab chow and water ad libitum. Mice were sacrificed by CO_2

asphyxiation and cervical dislocation. The colorectum was removed, opened longitudinally on a chilled glass plate and washed with ice-cold saline. Colons were gently scraped with sterile RNase and DNase-free microscope slides to remove the mucosal cells. Approximately half of the mucosal cells from each animal were placed directly into RNA isolation buffer for immediate RNA isolation, and the other half was flash frozen in liquid nitrogen for DNA isolation.

In a follow up study, mouse tissue samples for the folate level determination were obtained from Dr. Richard A. Miller's lab at the University of Michigan in Ann Arbor. BALB/cByJ3C57BL/6J F1 (CB6F1) females and C3H/HeJ3DBA/2J F1 (C3D2F1) males were mated to produce genetically heterogeneous populations in which each animal was genetically unique, but a full sibling of all other mice in the population (Harrison, Strong et al. 2009). Mice were anesthetized in a CO_2 chamber and sacrificed by cervical dislocation. Harvested colonic mucosa was flash frozen and stored in liquid nitrogen. Experiments were performed in young (4–6 months) and old (22–24 months) male specific pathogen-free mice.

Real-time RT-PCR transcript quantitation

Total RNAs were isolated from the colonic mucosa of young and old C57BL/6 and CB6XC3D2 mice using the VersaGene RNA Isolation Kit in the presence of TCEP reducing agent (Gentra, Minneapolis, MN). cDNAs were synthesized from 2 mg RNA using random hexamer primers and an RT-PCR kit (Perkin Elmer, Waltham, MA), and purified with the QIAquick PCR Purification Kit

(Qiagen, Valencia, CA). All transcripts were quantitated with a LightCycler real time PCR machine (Roche, Indianapolis, IN). PCR reactions contained 2 µg purified cDNA, 4 mM MgCl2, 0.5 mM each of sense and antisense primers, and 2 ml FastStart DNA Master SYBR Green I enzyme-SYBR reaction mix (Roche). Primer sequences are detailed in Table 2. For all amplifications, PCR conditions consisted of an initial denaturing step of 99 ºC for 10 min, followed by 35–55 cycles of 96 ºC for 10 s, 62 ºC for 10 s and 72 ºC for 5 s, with a melting curve analysis from 40 ºC to 99 ºC to confirm specificity. External standards were prepared by amplification of cDNAs for each gene using the above primers. The amplicons were cloned into pGEM-T Easy vector, the vectors were linearized with ApaI and used to prepare external standard curves. All transcripts were normalized to either GAPDH or 18S RNA. Results are expressed as mean values from 2 to 3 separate experiments. Data were analyzed prior to normalization to ensure that normalization did not alter the direction or magnitude of differential transcript abundance between groups.

Folate level determination by folate microbiological assay

Folate levels were determined using *Lactobacillus casei* folate assay as described in Chapter 2. The mice colonic mucosa samples were weighted, added 10vol Buffer #1, then were homogenized (Pellet pestle Motor, Kontes) 20 times or until the solution was even. Samples were centrifuged at 12000rpm for 30 min. Supernatants were transferred to new tube and added 0.2 vol Buffer #2. Then they were incubated in the boiling water bath for 5 minutes, and centrifuged at

12000rpm for 5 minutes. Supernatants were transferred to new tube with 20µl of conjugase (chicken pancreas powder lyophilized, Pel-Freez, Rogers, Arkansas) and 80µl of Buffer #1 for the conjugase treatment. The control consisted of 160 µl of Buffer #1, 20µl conjugase, and 20µl Buffer #2. Samples were incubated in a 32ºC water bath for four hours. After flash freezing, the samples were stored in -80 ºC for next day folate microbiological assay use.

The tissue folate levels were measured using the *Lactobacillus casei* (ATCC 7469) microbiological assay, modified from Horne et al (Horne and Patterson 1988). Briefly, *L. casei* is cultured overnight in growth media (4.7% w/v solution Folic Acid Casei Medium, DifcoTM, Becton Dickinson, Sparks, MD) supplemented with 0.025% sodium ascorbate and 0.6µg/L folinic acid calcium salt (Santa Cruz, Santa Cruz, CA) to an OD of 0.05. The 300 µl reaction mixture contains 150µl media (9.4% solution Folic Acid Casei Medium, DifcoTM Becton Dickinson, Sparks, MD; 0.05% w/v sodium ascorbate), 8µl working buffer (0.16% w/v sodium ascorbate; 0.05mol/L potassium phosphate, pH 6.1), tissue homogenized solution (1µl, 2µl and 10µl for each sample) or the folinic acid calcium salt as standard (0, 10,20,40,60,80,100,120 fmol in each well), and at the end load 20µl *L.casei* at OD=0.05. A range of sample volumes are used to ensure data fall within standard curve range. Sterile water is used to adjust final volume to 300µl. The light-sensitive samples are covered and incubated at 37˚C for 21hrs. Absorbance is read at 595nm using a Genios Basic TECAN-GENios plus plate reader and TECAN Magellan v6.00 software (Tecan Group Ltd., Zurich, Switzerland). Folate concentration is calculated by comparing with standard.

Folate concentration is considered significantly different from control at a p-value < 0.05.

Uracil detection

Uracil in DNA was detected as previously described (Cabelof et al., 2006a and Cabelof et al., 2006b). Briefly, DNA was isolated from colon mucosal scrapings using Qiagen (Valencia, CA) gravity tip columns per manufacturer's protocol. Briefly, 4 µg DNA was blocked for 2 h at 37 °C in a tris/methoxyamine buffer (100 mM methoxyamine (Sigma–Aldrich, St Louis, MO) and 50 mM Tris–HCl, pH 7.4). DNA was precipitated with 7.5% volumes of 4 M NaCl and 4 volumes ice-cold 100% ethanol and re-suspended in TE buffer, pH 7.6. DNA was then treated with 0.4 units Uracil DNA Glycosylase (New England Biolabs, Ipswich, MA) for 15 min at 37 °C, immediately precipitated and re-suspended in TE buffer, pH 7.6. DNA was then probed with 2 mM aldehydic reactive probe (Dojindo Molecular Technology, Rockville, MD) for 15 min at 37 °C followed by ethanol precipitation and re-suspension in TE buffer. DNA was then heat denatured, immobilized onto a nitrocellulose membrane (Schleicher and Schuell, Dassel, Germany), and baked under vacuum. The dried membrane was washed in 5× SSC for 15 minutes at 37 °C, then incubated in a prehybridization buffer (20 mM Tris, pH 7.5; 0.1 M NaCl; 1 mM EDTA; 0.5% casein w/v; 0.25% BSA w/v; and 0.1% Tween-20 v/v for 30 min at room temperature). Streptavidin-POD conjugate (Roche, Indianapolis, IN) was added at a 1:2000 dilution for 45 min at room temperature. Membrane was washed in TBS/Tween-20 three times at

37 °C, incubated in ECL solution (Pierce-Thermo Fisher, Rockford, IL) for 5 minutes at room temperature, then visualized and quantified using a ChemiImager™ system (Alpha Innotech-Protein Simple, Santa Clara, CA). Data are expressed as the integrated density value of the band per microgram of DNA loaded on the membrane.

Statistical Analysis

Differences between 7~10 young and 8~10 old mice were analyzed using Student's *t*-test. A *p*-value of < 0.05 was considered significantly different. *P* values of < 0.05 and *P* values of < 0.01 are presented. Data are presented as means ± SEMs. All statistics were performed using Microsoft excel.

RESULTS

Folates are essential for cell survival due to their function in carrying and transferring one-carbon units in biosynthesis pathways. Because the mammalian cells cannot make folate *de novo*, cells have to obtain the folate from the diet. The folic acid from the diet is absorbed in the small intestine, and is transported by the reduced folate carrier (RFC) through the cell membrane and into the cell. Then it is reduced to dihydrofolate, which is reduced by the enzyme dihydrofolate reductase (DHFR) to tetrahydrofolate (polyglutamate) using NADPH as electron donor. Tetrahydrofolate with poly-glutamate residues tail retains folate inside the cells and make it possible to do the bio-functions in cells. When the poly-glutamate tail is hydrolyzed by Gamma-glutamyl hydrolase (GGH), the molecule

will become monoglutamated, allowing transport out of the cells (Shen, Rothman et al. 2005). There are plenty of folate transport systems, including: uptake and export. The uptake proteins include: membrane-localized folate-binding proteins (FBPs), RFC, and a low pH folate transporter. The export proteins include multidrug resistance proteins (MRPs). We showed increased RFC transcription results increased transport of folate from the lumen into the enterocyte (Liu, Ge et al. 2005). In our study, we determined the RFC transcription levels, and found over 2 fold up-regulation in old mice colon (Figure 24). We explained under the aging condition, the cells try to take more folate into the cells. Also we found the transcription levels of GGH and MRP3 are significantly down-regulated in old mouse colon (Figure 24). These are consistent with the RFC data, showing the old mice colon cells try to lose as little folate as they can. We explain that the colon cells in aging condition are trying to keep more folate in cells for their survival. Liu et al. also showed whole-body folate deficiency induces the folate exporter genes expression GGH and MRP3 (Liu, Ge et al. 2005). We are very curious to know what happens to the folate level in old mice colon. Due to the animal tissues availability, we didn't detect the folate level in the same tissue with the detection of folate transporters genes. We detected the folate level in the colon tissues (CB6XC3D2 mice). In spite of reports that colonic folate levels decrease with age (Choi, Friso et al. 2003), we found the folate level in old colon slightly decreased but not significantly. (Figure 25).

Uracil DNA glycosylase gene expression and uracil accumulation are altered with age. The uracil level in DNA is related not only to how much

misincorporated uracil is in DNA, but also to how much the uracil DNA glycosylases remove the uracil base from DNA. We determined the uracil level in old colon and found about 30% significant increased uracil in old colon than in young colon (Figure 27). Aging induces uracil accumulation in mouse colon tissue. Interestingly, when we evaluated the transcription level of Ung and Smug1, which are the most crucial enzymes to remove uracil from deaminated cytosine or opposite to adenine during DNA replication, the results show there are about 2-2.5 fold increase for both uracil DNA glycosylases in old colon (Figure 26). We explained those results that in the old mice colon tissue, uracil accumulation in DNA response to aging, which leads the colon to try to adopt the ability to remove the uracil from DNA and protect the cells to survive. But the removal ability is not up-regulated enough; there is still some uracil kept in DNA and persisting at greater levels than in young colon tissues.

CONCLUSION

Aging impact on the folate metabolism genes

While folate depletion with age have been reported (Choi, Friso et al. 2003, Jimenez-Redondo, Beltran de Miguel et al. 2014), ours was the first observation that folate transporters and folate retention enzymes are likewise altered with age. Once absorbed, the folate will go through cell membranes by folate transporters, including RFC and MRP3. And the polyglutamate and monoglutamate forms of folate will interconvert through the enzymes GGH and FPGS catalyzation, which will maintain the folate homeostasis in cells. As expected, in our study, in

response to age in the colon, the folate metabolism status has changed. The intake folate transporter RFC gene expression is up-regulated, and the enzymes, GGH and MRP3, which help to export folate from cells are down-regulated. With aging, it seems the colon tissues adapt the folate metabolism mechanism and try to maintain the folate inside the colon cells. That explained the folate level has no significant difference between the young and old mice colon in our study. In particular, Choi et al. (Choi, Friso et al. 2003) evaluated whole body and tissue specific folate status in rats at approximately 4 months and 18 months and found that animals maintained on folate replete diets exhibited no evidence of whole body folate depletion (plasma indicators), but did display evidence of folate depletion within the old colon (increased uracil, reduced folate status). Within the framework of this animal model and sample availability, we are unable to further evaluate this question, but it raises questions worthy of further investigation. In future direction, we will evaluate the folate transport enzymes including RFC, FBPs, MRPs, GGH et al. in rats to see if colonic folate depletion in old rats results from inability to maintain folate levels in colonic mucosa.

Aging impact on uracil accumulation in mice colon
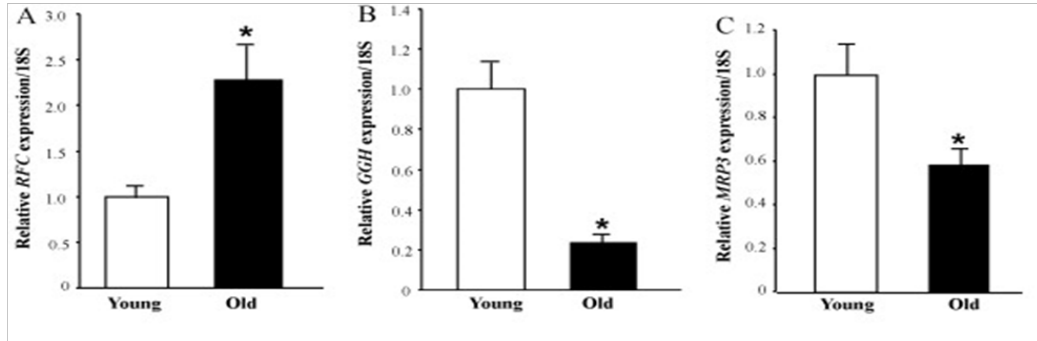
In this work, we found that the increase in *Ung* and *Smug1* expression is 2–2.5 fold in old colons. However, in spite of this relatively large increased expression of uracil-removing enzymes, we are still able to detect a small increase in uracil in DNA. In the earlier study of experimental folate depletion, we didn't find the uracil accumulation in DNA of BNLC2 cells (Chapter 3). And we

found the up-regulated *Ung* gene expression (~5 fold) and UDG activity (~2 fold). The increased uracil removal by UDG is efficient enough to clear uracil from DNA, then we didn't find uracil accumulation under the folate depletion condition. Due to the cell specific response to the folate deficiency, in MEF cells, uracil accumulation was observed, and no up-regulation of *Ung* gene expression was observed. The ability of uracil removal in MEFs is not efficient enough to clear uracil from DNA. Also we were unable to detect increased DNA uracil levels in liver, and found the up-regulated expression and activity of uracil-excising enzymes in liver (Cabelof, Raffoul et al. 2004). All these suggest that whether we are able to detect uracil accumulation depends on the ability of removal of misincorporated uracil. Also these data suggest a high level of uracil incorporation in mice colon under aging condition. The increased uracil removal ability (2.5 fold < 5 fold) are not sufficient to remove the high level of uracil misincorporated in the old mice colon. In Choi's study (Choi, Friso et al. 2003), 30~45% lower colonic folate and 50% higher colonic uracil in old rats than in young rats were observed. And they concluded the elder rats are more susceptible to biochemical and molecular consequences of folate depletion than that of young rats. That also describes the tissue specific phenotype of the uracil process to the aging.

Interestingly, Kim et al. (Kim, Jang et al. 2011), did not observe differences of uracil misincorporation in DNA in the same folate dietary groups between the young and old in colon and even in liver of C57BL/6 mice. Also, their liver folate concentration data didn't show significant differences between the

young and old mice (old: 9.27 µg/g tissue; young: 10.90 µg/g tissue). The mice they used are 4months and 18months old. In our study we used the same mouse model (C57BL/6) with 4~6months and 24~28months old. The 6~10 months elder in the age of mice maybe can explain the different results of the uracil misincorparation in DNA and the folate status. That makes us more curious about the colonic folate level and colonic uracil process in the same old mice strain with same age.

Figure 24: Aging impact on the expression of folate transport enzymes in mouse colonic mucosa. A. *RFC* expression in aged colonic mucosa. cDNAs were prepared from RNA isolated from colonic mucosa of 10 young (4–6 months) and 10 old (24–28 mon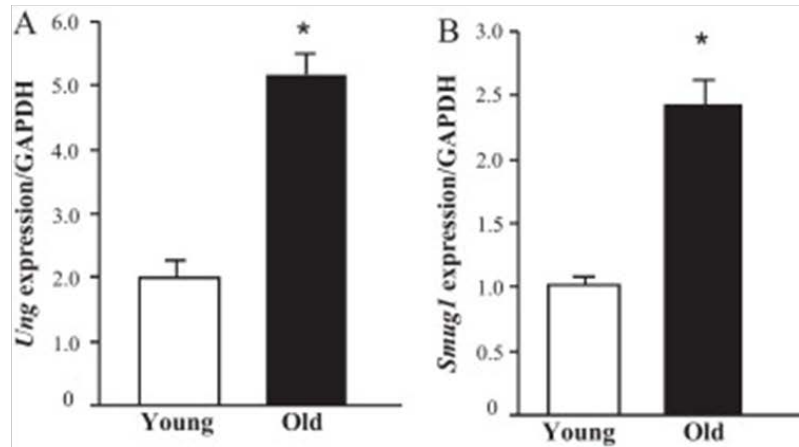ths) mice as described in methods. RFC transcript levels were determined by real time RT-PCR analysis and normalized to 18S rDNA. Data are presented as mean ± SEM. Normalized and unnormalized data are equivalent. B. cDNAs were prepared from RNA isolated from colonic mucosa of 10 young (4–6 months) and 10 old (24–28 months) mice as described in methods. GGH transcript levels were determined by real time RT-PCR analysis and normalized to 18S rDNA. Data are presented as mean ± SEM. Normalized and unnormalized data are equivalent. C. cDNAs were prepared from RNA isolated from colonic mucosa of 10 young (4–6 months) and 10 old (24–28 months) mice as described in methods. MRP3 transcript levels were determined by real time RT-PCR analysis and normalized to 18S rDNA. Data are presented as mean ± SEM. Normalized and un-normalized data are equivalent. *All values significantly different from control at $p < 0.01$.

Aging impact on the folate level in mouse colonic mucosa
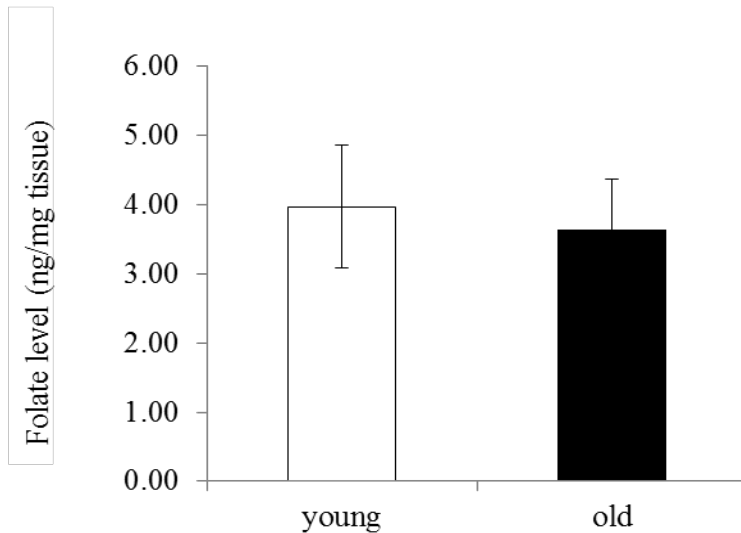
Figure 25: Aging impact on the folate level in mouse colonic mucosa. The folate level slightly decreases in the old mice colon tissue. BALB/cByJ3C57BL/6J F1 (CB6F1) females and C3H/HeJ3DBA/2J F1 (C3D2F1) males were mated to produce genetically heterogeneous populations in which each animal was genetically unique, but a full sibling of all other mice in the population. Experiments were performed in 9 young (4–6 months) and 9 old (22–24 months) male specific pathogen-free mice.

Aging impact on the expression of uracil-excising enzymes in mouse colonic mucosa

Figure 26: Aging impact on the expression of uracil-excising enzymes in mouse. Expression of uracil-excising enzymes increases with age. cDNAs were prepared from RNA isolated from colonic mucosa of 10 young (4–6 months) and 10 old (24–28 months) mice as described in methods. (A) Ung transcript levels were determined by real time RT-PCR analysis and normalized to *GAPDH*. Data are presented as mean ± SEM. Normalized and unnormalized data are equivalent. (B) Smug transcript levels were determined by real time RT-PCR analysis and normalized to *GAPDH*. Data are presented as mean ± SEM. Normalized and un-normalized data are equivalent. *All values significantly different from control at p < 0.01.

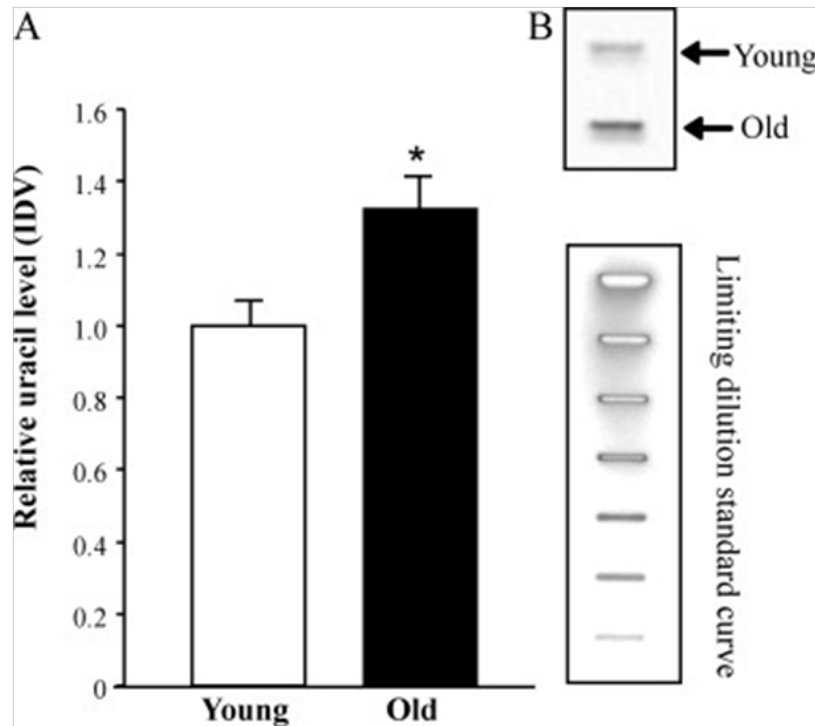## Aging impact on the accumulation of uracil in mouse colon DNA

Figure 27: Aging impact on the accumulation of uracil in mouse colon DNA.

A. DNA was isolated from colonic mucosa of 7 young (4–6 months) and 8 old (24–28 months) mice and uracil levels were detected as described in methods. Data are presented as mean ± SEM. Uracil levels are determined by integrated density volume (IDV); values in the young (control group) establish the baseline value of 1.0. B. Representative image of colonic uracil accumulation in young (top) and old (bottom). A standard curve made from limiting 2-fold dilutions of bisulfite-treated DNA is shown.

CHAPTER 5

FUTURE DIRECTIONS

Folate is a critical nutrient with important implications for health. Folate deficiency may cause loss of appetite, loss of weight, weakness, headaches, heart palpitations, behavioral disorders, anemia, slow growth rate of children, low birth weight and premature infants, neural tube defects in infants, depression, and also many chronic diseases which are commonly found among the aging people, such as cardiovascular disease and tumor/cancer. Folate has important biological functions in the one-carbon unit transport, among them the nucleotide synthesis and DNA methylation have key relationships with the folate-related carcinogenesis (Jang, Mason et al. 2005).

Folate deficiency and uracil misincorporation in DNA has been studied for many years. The limited one-carbon units result in the dUMP/dTMP ratio imbalance, which may cause the uracil accumulation in DNA. As our data show, MEF cells grow without folate in media persist 1.4 fold level of uracil compared with the control group. The misincorporated uracil in DNA is processed by the DNA base excision repair (BER). In different tissue or cell lines, the DNA glycosylase gene expression and enzyme activity may be different, which may lead to different BER activities among tissues/cells. Our data of BNLC2 liver cells in the folate depletion condition have shown increased DNA glycosylase expression and activity of UNG which is different from what we observed in MEFs. And we didn't find DNA uracil accumulation in BNLC2. This is similar to

the results we found in the whole animal, in which in the liver, uracil did not accumulate in DNA in response to folate depletion. We suggest that uracil DNA glycosylase up-regulation prevents the uracil accumulation in the folate depletion status, and our data support this hypothesis.

A previous study (Choi, Friso et al. 2003) showed that in the 1 year old male Sprague-Dawley rat colon, there is 50% more uracil in DNA than in weanling rats, and 35~45% less folate than in young rats by the affinity/HPLC method. We compared the DNA uracil level in the young (4-6 months) and old (24-28 months) male C57BL/6 mouse colon, and found about 30% DNA uracil level higher in old than in young. Also we found the folate transporter enzymes' (RFC, GGH, MRPS) gene expression level are up-regulated in the old mice; that may be explained by the old mice trying to retain folate inside the colon tissue. Due to the limiting amount of colon epithelial tissue, we were unable to determine the folate status directly in this study. Instead, we were able to obtain young and old colons for folate status determination in heterogenous laboratory male mice generated by crossing CB6F1 female and C3D2F1 male mice. Here we found the folate level slightly decreased by 10% in the old (22-24 months) mice compared with the young (4-6 months) mice by the microbiological *Lactobacillus casei* assay, though the difference was not significant. We evaluated the mRNA level of the uracil DNA glycosylase and found there is about 2.5 fold increase of *UNG* and *Smug*1 in the old mice. Though the loss of folate in old colon tissue is not a robust finding, we still observe an impact of aging on *Ung* and *Smug* levels, suggesting a similar compensatory response to folate depletion seen in the

tissue culture models. We are unable to draw any definitive conclusions based solely on these data, but the data gave us more interest in the relationship between the folate status and aging. Both of folate status and aging may alter the DNA repair ability, which may result in DNA mutation, damages in chromosomes, and cause various diseases and carcinogenesis.

In order to firmly establish a role for *Ung* in the phenotype of DNA uracil accumulation in response to folate depletion, we will also need to evaluate these questions in other DNA uracil-excising glycosylase deficient models. Based on our findings here, we do not suspect that *Smug, TDG, or MBD4* null genotypes will impact uracil accumulation. It is also potentially interesting to consider combining *Ung* and *Smug* null genotypes to evaluate the impact of folate response on uracil accumulation.

In the future, we will compare the folate status in the same tissue/cells between various methods, and try to figure out the relationship between the convenient microbiological *Lactobacillus casei* assay and other methods such as HPLC and protein binding assay. This will be a big stone in the folate assay fields and make it possible to compare the results between different research labs or projects.

Also, we will study the protein levels of the multiple enzymes involved in DNA base excision repair pathway and compare them with protein activity to confirm the UNG functions in the prevention of the uracil accumulation in

response to the folate depletion. And, if we can get data from MEFs *TDG*-KOs and *MBD4*-KOs as described above, our story may get more support.

Uracil in DNA is not the only target substrate of BER. There are many base lesions that are BER substrates. 8-oxoguanine (8-oxoG) is a mutagenic base that occurs as a result of exposure to reactive oxygen species (ROS), and is an important target substrate of BER. It may be removed by 8-oxoguanine glycosylase (OGG1). We found that folate depletion has no significant effect on the BER activity with 8-oxo-G substrate in MEFs (*UNG*$^{+/+}$) (Figure 28). Also we compared the 8-oxo-G BER ability between the MEFs (*UNG*$^{+/+}$) and MEFs (*UNG*$^{-/-}$). Surprisingly, we found UNG knocked out cells have significantly reduced ability to repair the 8-oxo-guanine (Figure 29). That made us curious whether UNG and OGG1 have some interaction during the BER. If we give back UDG during the reaction, will the OGG1 BER function be backup or not? Those questions may open a new window for us to look at folate and DNA repair.

ACKNOWLEDGEMENTS

We are appreciative for the mouse blood sample donation from Dr. Ahmad Heydari from Wayne State University and the mouse tissue samples from Dr. Richard A. Miller at the University of Michigan.

Effect of folate depletion on BER activity with 8-oxo-G substrate
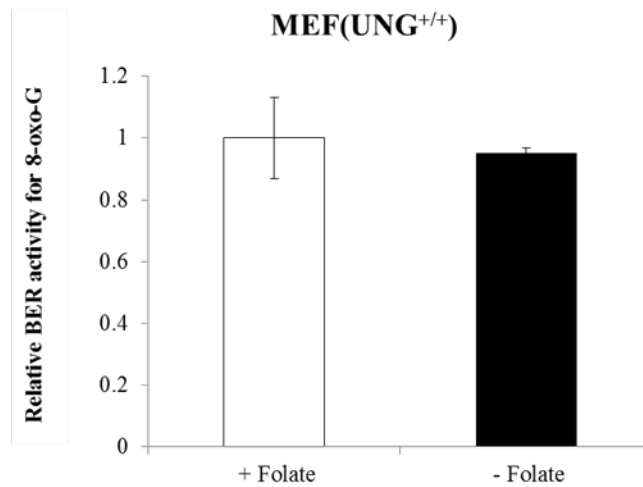
Figure 28: Effect of folate depletion on BER activity with 8-oxo-G substrate.

Folate depletion has no significant effect on BER activity with 8-oxo-G substrate in MEFs($UNG^{+/+}$) cells. BER activity was determined in cells grown in the presence and absence of folate as described in Methods. There are 4 samples in each group.
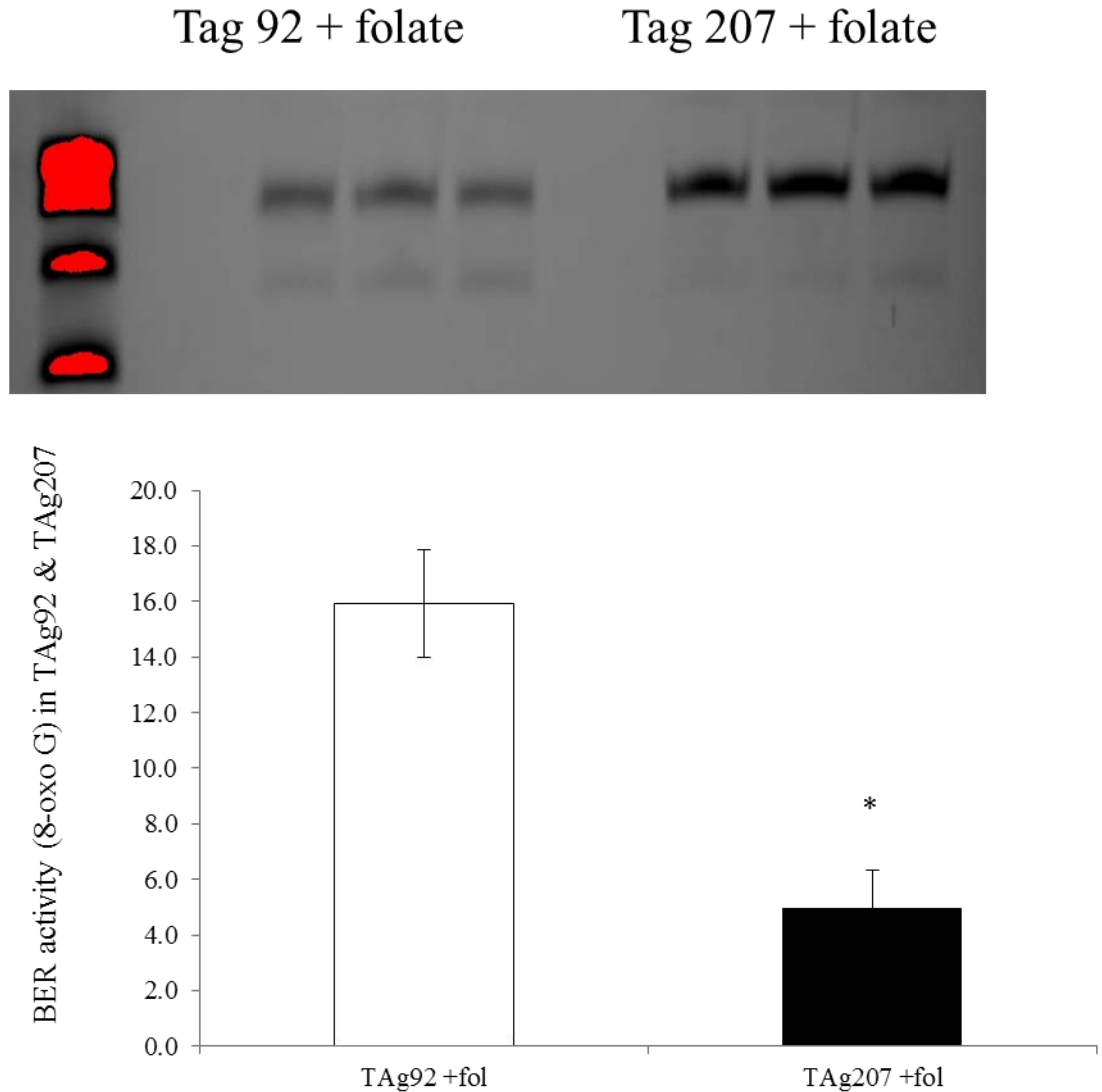
Figure 29: 8-oxoguanine is removed by OGG1 during BER activity. This BER activity is significantly down regulated when the UNG is knocked out in the MEF cells. There are 4 samples in each group. Tag92: MEFs ($UNG^{+/+}$); Tag207: MEFs ($UNG^{-/-}$). *: P value < 0.05.

REFERENCES

Alberts, B. (2002). <u>Molecular biology of the cell</u>. New York, Garland Science.

An, Q., P. Robins, T. Lindahl and D. E. Barnes (2005). "C --> T mutagenesis and gamma-radiation sensitivity due to deficiency in the Smug1 and Ung DNA glycosylases." <u>EMBO J</u> **24**(12): 2205-2213.

Appaji Rao, N., M. Ambili, V. R. Jala, H. S. Subramanya and H. S. Savithri (2003). "Structure-function relationship in serine hydroxymethyltransferase." <u>Biochim Biophys Acta</u> **1647**(1-2): 24-29.

Beetstra, S., P. Thomas, C. Salisbury, J. Turner and M. Fenech (2005). "Folic acid deficiency increases chromosomal instability, chromosome 21 aneuploidy and sensitivity to radiation-induced micronuclei." <u>Mutat Res</u> **578**(1-2): 317-326.

Blancquaert, D., S. Storozhenko, K. Loizeau, H. De Steur, V. De Brouwer, J. Viaene, S. Ravanel, F. Rebeille, W. Lambert and D. Van Der Straeten (2010). "Folates and Folic Acid: From Fundamental Research Toward Sustainable Health." <u>Critical Reviews in Plant Sciences</u> **29**(1): 14-35.

Blount, B. C., M. M. Mack, C. M. Wehr, J. T. MacGregor, R. A. Hiatt, G. Wang, S. N. Wickramasinghe, R. B. Everson and B. N. Ames (1997). "Folate deficiency causes uracil misincorporation into human DNA and chromosome breakage: implications for cancer and neuronal damage." <u>Proc Natl Acad Sci U S A</u> **94**(7): 3290-3295.

Branda, R. F., J. P. O'Neill, E. M. Brooks, C. Powden, S. J. Naud and J. A. Nicklas (2007). "The effect of dietary folic acid deficiency on the cytotoxic and mutagenic responses to methyl methanesulfonate in wild-type and in 3-

methyladenine DNA glycosylase-deficient Aag null mice." <u>Mutation Research-Fundamental and Molecular Mechanisms of Mutagenesis</u> **615**(1-2): 12-17.

Bull, C. F., G. Mayrhofer, N. J. O'Callaghan, A. Y. Au, H. A. Pickett, G. K. Low, D. Zeegers, M. P. Hande and M. F. Fenech (2014). "Folate Deficiency Induces Dysfunctional Long and Short Telomeres; Both States Are Associated with Hypomethylation and DNA Damage in Human WIL2-NS Cells." <u>Cancer Prev Res (Phila)</u> **7**(1): 128-138.

Cabelof, D. C., J. Nakamura and A. R. Heydari (2006). "A sensitive biochemical assay for the detection of uracil." <u>Environ Mol Mutagen</u> **47**(1): 31-37.

Cabelof, D. C., J. J. Raffoul, J. Nakamura, D. Kapoor, H. Abdalla and A. R. Heydari (2004). "Imbalanced base excision repair in response to folate deficiency is accelerated by polymerase beta haploinsufficiency." <u>J Biol Chem</u> **279**(35): 36504-36513.

Choi, S. W., S. Friso, G. G. Dolnikowski, P. J. Bagley, A. N. Edmondson, D. E. Smith and J. B. Mason (2003). "Biochemical and molecular aberrations in the rat colon due to folate depletion are age-specific." <u>J Nutr</u> **133**(4): 1206-1212.

Clarke, R., A. D. Smith, K. A. Jobst, H. Refsum, L. Sutton and P. M. Ueland (1998). "Folate, vitamin B12, and serum total homocysteine levels in confirmed Alzheimer disease." <u>Arch Neurol</u> **55**(11): 1449-1455.

Courtemanche, C., I. Elson-Schwab, S. T. Mashiyama, N. Kerry and B. N. Ames (2004). "Folate deficiency inhibits the proliferation of primary human CD8+ T lymphocytes in vitro." <u>J Immunol</u> **173**(5): 3186-3192.

Dominic Taylor, P. M. "Folic acid , a necessary ingredient for building DNA, cells and babies." University of Bristol, Bristol, UK.

Duthie, S. (1999). "Folic acid deficiency and cancer: mechanisms of DNA instability." British Medical Bulletin **55**(3): 5.

Duthie, S. J., G. Horgan, B. de Roos, G. Rucklidge, M. Reid, G. Duncan, L. Pirie, G. P. Basten and H. J. Powers (2010). "Blood folate status and expression of proteins involved in immune function, inflammation, and coagulation: biochemical and proteomic changes in the plasma of humans in response to long-term synthetic folic acid supplementation." J Proteome Res **9**(4): 1941-1950.

Fenech, M. (2001). "The role of folic acid and Vitamin B12 in genomic stability of human cells." Mutat Res **475**(1-2): 57-67.

Fenech, M. (2012). "Folate (vitamin B9) and vitamin B12 and their function in the maintenance of nuclear and mitochondrial genome integrity." Mutat Res **733**(1-2): 21-33.

Gartel, A. L. and S. K. Radhakrishnan (2005). "Lost in transcription: p21 repression, mechanisms, and consequences." Cancer Res **65**(10): 3980-3985.

Ghandour, H., B. F. Lin, S. W. Choi, J. B. Mason and J. Selhub (2002). "Folate status and age affect the accumulation of L-isoaspartyl residues in rat liver proteins." J Nutr **132**(6): 1357-1360.

Harrison, D. E., R. Strong, Z. D. Sharp, J. F. Nelson, C. M. Astle, K. Flurkey, N. L. Nadon, J. E. Wilkinson, K. Frenkel, C. S. Carter, M. Pahor, M. A. Javors, E. Fernandez and R. A. Miller (2009). "Rapamycin fed late in life extends lifespan in genetically heterogeneous mice." Nature **460**(7253): 392-395.

Henderson, G. B., M. R. Suresh, K. S. Vitols and F. M. Huennekens (1986). "Transport of folate compounds in L1210 cells: kinetic evidence that folate influx proceeds via the high-affinity transport system for 5-methyltetrahydrofolate and methotrexate." Cancer Res **46**(4 Pt 1): 1639-1643.

Herrmann, W., S. Quast, M. Ullrich, H. Schultze, M. Bodis and J. Geisel (1999). "Hyperhomocysteinemia in high-aged subjects: relation of B-vitamins, folic acid, renal function and the methylenetetrahydrofolate reductase mutation." Atherosclerosis **144**(1): 91-101.

Horne, D. W. and D. Patterson (1988). "Lactobacillus casei microbiological assay of folic acid derivatives in 96-well microtiter plates." Clin Chem **34**(11): 2357-2359.

Jacobs, A. L. and P. Schar (2012). "DNA glycosylases: in DNA repair and beyond." Chromosoma **121**(1): 1-20.

James, S. J., M. Pogribna, I. P. Pogribny, S. Melnyk, R. J. Hine, J. B. Gibson, P. Yi, D. L. Tafoya, D. H. Swenson, V. L. Wilson and D. W. Gaylor (1999). "Abnormal folate metabolism and mutation in the methylenetetrahydrofolate reductase gene may be maternal risk factors for Down syndrome." Am J Clin Nutr **70**(4): 495-501.

Jang, H., J. B. Mason and S. W. Choi (2005). "Genetic and epigenetic interactions between folate and aging in carcinogenesis." J Nutr **135**(12 Suppl): 2967S-2971S.

Jennings, B. A. and G. Willis (2014). "How folate metabolism affects colorectal cancer development and treatment; a story of heterogeneity and pleiotropy." Cancer Lett.

Jimenez-Redondo, S., B. Beltran de Miguel, J. Gavidia Banegas, L. Guzman Mercedes, J. Gomez-Pavon and C. Cuadrado Vives (2014). "Influence of nutritional status on health-related quality of life of non-institutionalized older people." J Nutr Health Aging **18**(4): 359-364.

Johansson, M., P. N. Appleby, N. E. Allen, R. C. Travis, A. W. Roddam, L. Egevad, M. Jenab, S. Rinaldi, L. A. Kiemeney, H. B. Bueno-de-Mesquita, S. E. Vollset, P. M. Ueland, M. J. Sanchez, J. R. Quiros, C. A. Gonzalez, N. Larranaga, M. D. Chirlaque, E. Ardanaz, S. Sieri, D. Palli, P. Vineis, R. Tumino, J. Linseisen, R. Kaaks, H. Boeing, T. Pischon, T. Psaltopoulou, A. Trichopoulou, D. Trichopoulos, K. T. Khaw, S. Bingham, G. Hallmans, E. Riboli, P. Stattin and T. J. Key (2008). "Circulating concentrations of folate and vitamin B12 in relation to prostate cancer risk: results from the European Prospective Investigation into Cancer and Nutrition study." Cancer Epidemiol Biomarkers Prev **17**(2): 279-285.

Kim, K. C., H. Jang, J. Sauer, E. M. Zimmerly, Z. Liu, A. Chanson, D. E. Smith, S. Friso and S. W. Choi (2011). "Folate supplementation differently affects uracil content in DNA in the mouse colon and liver." Br J Nutr **105**(5): 688-693.

Kronenberg, G., C. Harms, R. W. Sobol, F. Cardozo-Pelaez, H. Linhart, B. Winter, M. Balkaya, K. Gertz, S. B. Gay, D. Cox, S. Eckart, M. Ahmadi, G. Juckel, G. Kempermann, R. Hellweg, R. Sohr, H. Hortnagl, S. H. Wilson, R. Jaenisch and M. Endres (2008). "Folate deficiency induces neurodegeneration

and brain dysfunction in mice lacking uracil DNA glycosylase." J Neurosci **28**(28): 7219-7230.

Lanska, D. J. (2010). "Chapter 30: historical aspects of the major neurological vitamin deficiency disorders: the water-soluble B vitamins." Handb Clin Neurol **95**: 445-476.

Le Leu, R. K., G. P. Young and G. H. McIntosh (2000). "Folate deficiency diminishes the occurrence of aberrant crypt foci in the rat colon but does not alter global DNA methylation status." J Gastroenterol Hepatol **15**(10): 1158-1164.

Liu, J., R. Pickford, A. P. Meagher and R. L. Ward (2011). "Quantitative analysis of tissue folate using ultra high-performance liquid chromatography tandem mass spectrometry." Anal Biochem **411**(2): 210-217.

Liu, M., Y. Ge, D. C. Cabelof, A. Aboukameel, A. R. Heydari, R. Mohammad and L. H. Matherly (2005). "Structure and regulation of the murine reduced folate carrier gene: identification of four noncoding exons and promoters and regulation by dietary folates." J Biol Chem **280**(7): 5588-5597.

Lu, L., J. Ni, T. Zhou, W. Xu, M. Fenech and X. Wang (2012). "Choline and/or folic acid deficiency is associated with genomic damage and cell death in human lymphocytes in vitro." Nutr Cancer **64**(3): 481-487.

Lucock, M. (2000). "Folic acid: nutritional biochemistry, molecular biology, and role in disease processes." Mol Genet Metab **71**(1-2): 121-138.

MacFarlane, A. J., D. D. Anderson, P. Flodby, C. A. Perry, R. H. Allen, S. P. Stabler and P. J. Stover (2011). "Nuclear localization of de novo thymidylate

biosynthesis pathway is required to prevent uracil accumulation in DNA." J Biol Chem **286**(51): 44015-44022.

Macfarlane, A. J., C. A. Perry, M. F. McEntee, D. M. Lin and P. J. Stover (2011). "Shmt1 heterozygosity impairs folate-dependent thymidylate synthesis capacity and modifies risk of Apc(min)-mediated intestinal cancer risk." Cancer Res **71**(6): 2098-2107.

McNulty, H., K. Pentieva, L. Hoey and M. Ward (2008). "Homocysteine, B-vitamins and CVD." Proc Nutr Soc **67**(2): 232-237.

Mitchell, H. K., E. E. Snell and W. R.J. (1941). "The concentration of "folic acid"." Journal of the American Chemical Society **63**.

Ries, L. A. G., Eisner, M.P., Kosary, C.L., Hankey, B.F., Miller, B.A., Clegg, L., Mariotto, A., Feuer, E.J. (Eds.), (2007). "SEER Cancer Statistics Review, 1975-2001. National Cancer Institute, Bethesda, MD." **2-1-07**.

Rodriguez, R. and M. Meuth (2006). "Chk1 and p21 cooperate to prevent apoptosis during DNA replication fork stress." Mol Biol Cell **17**(1): 402-412.

Said, H. M., N. Chatterjee, R. U. Haq, V. S. Subramanian, A. Ortiz, L. H. Matherly, F. M. Sirotnak, C. Halsted and S. A. Rubin (2000). "Adaptive regulation of intestinal folate uptake: effect of dietary folate deficiency." American Journal of Physiology-Cell Physiology **279**(6): C1889-C1895.

Sanjoaquin, M. A., N. Allen, E. Couto, A. W. Roddam and T. J. Key (2005). "Folate intake and colorectal cancer risk: a meta-analytical approach." Int J Cancer **113**(5): 825-828.

Shane, B. (2011). "Folate status assessment history: implications for measurement of biomarkers in NHANES." Am J Clin Nutr **94**(1): 337S-342S.

Shane, B. and E. L. Stokstad (1976). "Transport and utilization of methyltetrahydrofolates by Lactobacillus casei." J Biol Chem **251**(11): 3405-3410.

Shen, M., N. Rothman, S. I. Berndt, X. He, M. Yeager, R. Welch, S. Chanock, N. Caporaso and Q. Lan (2005). "Polymorphisms in folate metabolic genes and lung cancer risk in Xuan Wei, China." Lung Cancer **49**(3): 299-309.

Simon, K. W., H. Ma, A. A. Dombkowski and D. C. Cabelof (2012). "Aging alters folate homeostasis and DNA damage response in colon." Mech Ageing Dev **133**(2-3): 75-82.

Snell, E. E. and W. H. Peterson (1940). "Growth Factors for Bacteria: X. Additional Factors Required by Certain Lactic Acid Bacteria." J Bacteriol **39**(3): 273-285.

Song, J., A. Medline, J. B. Mason, S. Gallinger and Y. I. Kim (2000). "Effects of dietary folate on intestinal tumorigenesis in the apcMin mouse." Cancer Res **60**(19): 5434-5440.

Tamura, T., Y. S. Shin, M. A. Williams and E. L. Stokstad (1972). "Lactobacillus casei response to pteroylpolyglutamates." Anal Biochem **49**(2): 517-521.

Unnikrishnan, A., T. M. Prychitko, H. V. Patel, M. E. Chowdhury, A. B. Pilling, L. F. Ventrella-Lucente, E. V. Papakonstantinou, D. C. Cabelof and A. R. Heydari (2011). "Folate deficiency regulates expression of DNA polymerase beta in response to oxidative stress." Free Radic Biol Med **50**(2): 270-280.

Varela-Moreiras, G. and J. Selhub (1992). "Long-term folate deficiency alters folate content and distribution differentially in rat tissues." J Nutr **122**(4): 986-991.

Wani, N. A., A. Hamid and J. Kaur (2012). "Alcohol-associated folate disturbances result in altered methylation of folate-regulating genes." Mol Cell Biochem **363**(1-2): 157-166.

WHO (2012). Serum and red blood cell folate concentrations for assessing folate status in populations. Geneva, World Health Organization, 2012. Vitamin and Mineral Nutrition Information System.

ABSTRACT

URACIL ACCUMULATION RESPONSE TO FOLATE DEPLETION IS A FUNCTION OF DNA REPAIR IMBALANCE THAT MAY BE A MECHANISM OF AGING

by

Hongzhi Ma

August 2014

Advisor: Dr. Diane Cabelof

Major: Nutrition & Food Science

Degree: Doctor of Philosophy

Folate is an essential nutrient for humans. They carry and transfer one carbon units. They have important biological functions during many reactions, like DNA synthesis, RNA synthesis, DNA methylation, DNA repair, cell division and growth. Through biochemical techniques to determine the gene expression, enzyme activity, uracil level in DNA, and through microbiological assay to determine the folate level, elucidates mechanism of uracil accumulation response to folate depletion. The findings present how folate deficiency status affects the uracil DNA glycosylase activity, and uracil initiated DNA base excision repair. DNA repair ability decides whether there is uracil accumulation under the folate depletion condition in different cell lines. Further, there is uracil accumulation in the mice colon tissue found under the aging condition.

AUTOBIOGRAPHICAL STATEMENT

HONGZHI MA

I was born in Xinxiang, a middle city in China. I love science, arts and all kinds of sports. From elementary school to the high school I was always the top rank students. Beside the computer, physics, chemistry competition, I got the second awards of the national mathematics competition in high school. I have been the president of the students union for many years in the elementary school and did the student work until in my University. After five years study, I graduated from Shandong Medical University (now belong to Shandong University, top 20 in China) and got the Bachelor of medicine.

I came to USA with my husband and have two lovely children later. I got my master degree of the Library & Information Science from Wayne State University in 2004 and got the Miriam T. Larson Scholarship. In 2009 I joined the master program in the Nutrition & Food Science department, Wayne State University. Soon I changed to Ph.D program and was mentored by Dr. Diane Cabelof. During the four years in Dr. Cabelof's lab, I was studying the folate, folate metabolism, DNA base excising repair in cell culture and animal model. I am the second co-author for one research paper in Mechanisms of Aging and Development, and one review paper in Journal of Oncology. Also, during my Ph.D study, I have undergraduate teaching experience for nine semesters.